HYDRODYNAMIC ENTRANCE EFFECT ON BOILING AND NEAR CRITICAL HYDROGEN HEAT TRANSFER

by S. Stephen Papell and Dwight D. Brown

Lewis Research Center
Cleveland, Ohio 44135

NATIONAL AERONAUTICS AND SPACE ADMINISTRATION • WASHINGTON, D. C. • FEBRUARY 1971

1. Report No. NASA TN D-6159	2. Government Accession No.	3. Recipient's Catalog No.
4. Title and Subtitle HYDRODYNAMIC ENTRANCE EFFECT ON BOILING AND NEAR CRITICAL HYDROGEN HEAT TRANSFER		5. Report Date February 1971 6. Performing Organization Code
7. Author(s) S. Stephen Papell and Dwight D. Brown		8. Performing Organization Report No. E-5125
9. Performing Organization Name and Address Lewis Research Center National Aeronautics and Space Administration Cleveland, Ohio 44135		10. Work Unit No. 129-01 11. Contract or Grant No.
12. Sponsoring Agency Name and Address National Aeronautics and Space Administration Washington, D.C. 20546		13. Type of Report and Period Covered Technical Note 14. Sponsoring Agency Code

15. Supplementary Notes

16. Abstract

Heat transfer data were obtained from test sections designed with fully developed flow (straight) inlets and undeveloped flow (plenum) sharp edge inlets. In the boiling regime, inlet hydrodynamics influenced the transition from nucleate to film boiling over the entire test section length while film boiling was influenced up to about 4 to 8 diameters from the inlet. The near critical data showed that, in comparison to the fully developed inlet conditions, the plenum inlet could raise the heat transfer rates over the entire test section length with differences in the data increasing with heat flux and decreasing with Reynolds number. An equation that comprehends fully developed inlet flow, modified to correlate the plenum data, showed an average increase of 57 percent in the heat transfer rates.

17. Key Words (Suggested by Author(s)) Boiling Near critical Hydrogen Plenum inlet Straight inlet Heat transfer	18. Distribution Statement Unclassified - unlimited	
19. Security Classif. (of this report) Unclassified	20. Security Classif. (of this page) Unclassified	21. No. of Pages 48 22. Price* $3.00

*For sale by the National Technical Information Service, Springfield, Virginia 22151

HYDRODYNAMIC ENTRANCE EFFECT ON BOILING AND NEAR CRITICAL HYDROGEN HEAT TRANSFER

by S. Stephen Papell and Dwight D. Brown

Lewis Research Center

SUMMARY

Heat transfer data were obtained with cryogenic hydrogen flowing vertically through test sections designed with fully developed flow (straight) inlets and undeveloped flow (plenum) sharp edge inlets. The inlet hydrodynamics were found to influence the heat transfer in various degrees over the range of data that covers subcritical pressures from 35 to 100 psia (2.45×10^5 to 6.9×10^5 N/m^2 abs) and near critical pressures of 200 and 300 psia (13.8×10^5 and 20.7×10^5 N/m^2 abs); inlet velocity from 11 to 68 feet per second (3.4 to 20.7 m/sec); heat flux from 0.06 to 1.10 Btu/(sec)(in.^{2}) (9.8 to 180 W/cm^2).

In the subcritical regime, film boiling was influenced by the inlet conditions for a distance of 4 to 8 diameters downstream from the inlet. Within that limit, a wall temperature difference ranging from zero to about 100^o R (56 K) was observed depending on the heat flux level. At the higher heat fluxes, the plenum test section wall temperatures were greater than the straight inlet test section with the temperature difference decreasing to zero as the heat flux was reduced. At the lower heat fluxes a reversal in the data trend was noted with the inlet end of the plenum test section at a lower temperature than the straight inlet test secion. The transition from nucleate to film boiling was also found to be quite sensitive to the inlet hydrodynamics. The flow perturbation caused by the plenum inlet prevented the establishment of a vapor film at heat fluxes that supported film boiling in the straight inlet test section. This phenomenon was found to persist over the entire test section length with wall temperature differences of as much as 200^o R (111 K) existing under identical test conditions.

In the near critical heat transfer regime, data showed that in comparison to fully developed inlet conditions the plenum inlet could raise the heat transfer rates over the entire test section length ($x/d = 20$) with difference in the data increasing with heat flux and decreasing with Reynolds number. An equation from reference 3 designed to comprehend fully developed flow at the inlet of the test section was adapted to correlate the plenum inlet near critical data that were significantly influenced by inlet hydrodynamics. The modified equation yields an average increase of about 57 percent in the heat transfer rates.

INTRODUCTION

In recent years, significant numbers of experimental and analytical studies have been aimed at determining methods for predicting the heat transfer characteristics of cryogenic hydrogen. Experimental data were generated in various laboratories with facilities that had certain test similarities. The heat transfer sections were electrically (resistance) heated round tubes with geometrical variations limited to flow passage areas and heated lengths. A consistent boundary condition specified for these tests was an unheated hydrodynamic starting length that assured the existence of fully developed flow at the inlet of the heated portion of the test section. References 1 to 3 are examples of design correlations developed with data obtained under the test condition described previously.

For most practical applications, internal flow of this nature may be subject to various types of inlet conditions that could conceivably affect the heat transfer mechanisms involved. Examples of studies such as these are few in number and do not include data from the two-phase or near critical heat transfer regimes. A limited amount of data is presented in references 6 and 7 that describes forced convection heat transfer tests with water or air flowing through round tubes that are subject to inlet geometry perturbations. Orifices were located in the flow channels at the inlet of the heated portion of the test section to induce local flow separations. The data show a unique maximization in heat transfer some distance downstream of the inlet. Reference to these experimental results will be made later in this report.

The question raised in the present investigation is to what extent can boiling and near critical hydrogen heat transfer be influenced by relaxing the fully developed flow condition so that undeveloped flow could exist at the test section inlet? This type of hydrodynamic condition can conceivably exist at the entrance of a coolant channel in a regeneratively cooled rocket engine. The approach used was to compare data from two test sections with inlet geometries that induce large differences in hydrodynamic conditions.

One of the test sections contained a straight unheated inlet section that assured fully developed flow at the start of the heated length. The other test section contained a plenum directly in the flow channel that was positioned so that undeveloped flow existed through a sharp edge inlet at the start of the heated length. Both test sections were run under the same test conditions and data comparisons are presented in the body of this report. The range of data includes subcritical absolute pressures from 35 to 100 psi (2.4×10^5 to 6.9×10^5 N/m^2) and near critical absolute pressures of 200 and 300 psi (13.8×10^5 and 20.7×10^5 N/m^2), inlet velocities from 11 to 68 feet per second (3.4 to 20.7 m/sec), heat flux from 0.06 to 1.10 Btu/(sec)(in.^{2}) (9.8 to 180 W/cm^2), and inlet bulk temperatures from 43° to 48° R (24 to 27 K). The near critical regime investigated

herein is defined as fluid bulk inlet conditions that are above the critical pressure but below the critical temperature.

EXPERIMENTAL EQUIPMENT

Flow System

The experimental apparatus used to obtain both the boiling and the near critical heat transfer data is shown in figure 1. The system was composed of three integral units that include a helium gas high-pressure storage sphere mounted in an insulated cylindrical tank, a 40-gallon liquid hydrogen supply Dewar, and a cylindrical vacuum tank containing the test section, mixing chambers, and flow venturi.

The helium gas used to pressurize the liquid hydrogen Dewar was precooled by a liquid nitrogen bath to minimize heat transfer between the gas and the bulk liquid. The hydrogen flowed up the dip tube, through the test section, and then discharged to a piping system connected to a burn off torch. Upstream and downstream of the test section were mixing chambers designed to eliminate temperature stratification in the bulk fluid. Flow rates and system pressures were controlled by throttling valves located at the top of the Dewar and downstream of the test section tank. The entire flow system between the two control valves was vacuum jacketed to minimize external heat leaks. All data measurements were made within the vacuum test section tank.

Test Sections

Figure 2 schematically describes the physical dimensions and instrumentation locations of the two test sections used in this study. Both test sections were built with identical specifications except for variations in entrance geometry. The straight inlet test section had an unheated hydrodynamic starting length of about 30 diameters. The plenum test section had a sharp edge inlet (fig. 2(b)) with essentially a zero hydrodynamic starting length. A baffle plate in the plenum was used to break up the fluid jet with flow access through eight equally spaced, 1/4-inch- (0.64-cm-) diameter holes around the periphery of the plate.

An area change of 40 to 1 accelerated the fluid from nearly zero velocity in the plenum to velocities ranging from 11 to 68 feet per second (3.4 to 20.7 m/sec) at the inlet of the heating length. It is known that a flow contraction of this nature induces a vena contracta for some distance downstream. This flow separation is used to discuss some of the data phenomena presented later in this report.

The test sections were made of Inconel X tubing having an inside diameter of 0.311 inch (0.790 cm) and a wall thickness of 0.010 inch (0.025 cm). The heated portions of the test sections were 6.5 inches (16.5 cm) or about 21 diameters in length. The test sections were electrically isolated from the rest of the flow system by insulated bushings in the flange connections.

A uniform heat flux was generated with a 10 000-watt, 400-hertz alternator using the test section as a resistance heater. The power was controlled by a variable transformer that delivered a maximum of 16 volts and 600 amperes to the test section.

Instrumentation

Figure 3 shows the manner in which the test sections were installed within the vacuum tank. The flow path was down through a venturi meter and up through the instrumented test section. The outer surface temperatures of the test section (fig. 2(a)) were measured by 12 copper-constantan thermocouples made of 28-gage wire that were silver soldered in two rows 180° apart on the circumference of the tube. Five voltage taps made of 28-gage copper wire were installed along the tube to verify the linearity of the voltage drop. Fluid bulk temperature measurements were made with platinum resistance thermometers located in the mixing chambers. System pressures were also measured in the mixing chambers.

The power to heat the test sections was measured in terms of volts and amperes. The output signals were converted to low voltage direct current for recording purposes. These millivolt signals, along with the outputs of the pressure transducers, resistance thermometers and thermocouples were fed to a central data acquisition system and recorded on magnetic tape. The signals were isolated and split before going to the voltage digitizer and sent to a multichannel oscillograph for visual monitoring of the tests.

EXPERIMENTAL PROCEDURE

Calibrations were made prior to each run using standard instruments to assure measurement accuracy. The cooldown period was initiated by filling the liquid nitrogen bath tank within which the helium gas supply sphere was submerged. The 40-gallon (0.152-m^3) Dewar was then filled with liquid hydrogen while venting through the test section. The residual heat stored in both the Dewar and the flow system was removed in this manner. Auxiliary thermocouples (not shown in fig. 2) mounted on the electrodes of the test section were used as a cooldown guide. The cooldown and filling period was then followed by data acquisition through a systematic running procedure.

The controlled test variables were system pressure, fluid flow rate, and electrical power to generate the desired uniform heat fluxes. With the system pressure and flow rate set at some predetermined value, a data run was made by increasing the heat flux over a range of power inputs. Four discrete power settings were used for each data run. At each power setting sufficient time was allowed for steady-state conditions to prevail before the data were recorded. The tube wall temperatures, as viewed on the oscillograph were used as a stability guide. For some of the runs, at low flow rates, the wall temperature limited the amount of power that could be dissipated in the tube. Data runs were repeated over a range of fluid flow rates and system pressures.

The aforementioned running procedure was used for both the straight inlet and the plenum inlet test sections. Care was exercised to duplicate the test conditions so that data comparisons could be made.

The range of test conditions that were examined included subcritical absolute pressures from 35 to 100 psi (2.4×10^5 to 6.9×10^5 N/m^2) and near critical absolute pressures of 200 and 300 psi (13.8×10^5 and 20.7×10^5 N/m^2), inlet velocities from 11 to 68 feet per second (3.4 to 20.7 m/sec), heat fluxes from 0.06 to 1.10 Btu/(sec)(in.^{2}) (9.8 to 180 W/cm^2), and inlet bulk temperature between 43° and 48° R (24 and 27 K). The data are presented in tables I and II.

DATA ANALYSIS

The basic experimental data included measurements of electric power input, tube outer wall temperature, fluid flow rate, bulk temperature, and bulk pressure. The bulk measurements were inlet and exit mixing chamber values for both test sections. These measurements enabled the calculation of local heat transfer coefficients defined as

$$h_x = \frac{q}{T_i - T_b} \tag{1}$$

(All symbols are defined in the appendix.)

The heat flux q was obtained directly from voltage and current measurements assuming the heat leak from the outer wall of the test section to the vacuum environment and heat conduction along the wall as being negligible.

The tube wall temperature exposed to the fluid was calculated using the following equation obtained from reference 8, that assumes uniform internal power generation:

$$T_i = T_o - K\frac{Q}{k_m} \tag{2}$$

where

$$K = \frac{r_o^2 \ln \frac{r_o}{r_i} - \left(\frac{r_o^2 - r_i^2}{2}\right)}{2\pi L\left(r_o^2 - r_i^2\right)} \tag{3}$$

The local bulk temperature was obtained from the energy input to the fluid using a calculation procedure called subroutine STATE from reference 9. This was accomplished by consideration of the enthalpy rise of the fluid using the following equation that assumes sensible heating

$$H_{b,x} = H_{b,in} + \frac{Qx}{L\dot{\omega}} \tag{4}$$

The second term on the right side of the equation is the enthalpy rise of the fluid and was evaluated at each measuring station. Since enthalpy is a function of pressure and temperature, the bulk temperature can be obtained in this manner with a knowledge of the local pressure. The local pressure used for this calculation was the upstream mixing chamber value since the average pressure drop across both test sections of about 2 psi (0.07×10^5 N/m^2) was within measurement accuracy. This calculation was only made for the near critical data since it is not valid in the boiling regime when significant volumes of vapor are generated.

Local heat transfer coefficients as defined in equation (1) for the near critical data were then obtained using equations (2) to (4). Local Nusselt numbers were then calculated using h_x by the following relation:

$$Nu_x = \frac{h_x d}{k_w} \tag{5}$$

with thermal conductivity k evaluated at local bulk fluid conditions. Local Reynolds numbers were obtained as

$$Re_x = \frac{\rho V d}{\mu} \tag{6}$$

with absolute viscosity μ also evaluated at bulk conditions.

DATA COMPARISON AND DISCUSSION

The data that follow show the effect of hydrodynamic entrance conditions on boiling and near critical hydrogen heat transfer. Since the trends in the data were found to be unique in the different thermodynamic regimes, it will be convenient to treat each one separately.

Boiling (Two-Phase) Heat Transfer

The influence of hydrodynamic entrance conditions on boiling heat transfer is illustrated graphically in figure 4 which presents data for an absolute pressure of 50 psi (3.4×10^5 N/m^2) over a range of inlet bulk velocities. Data comparisons are made with temperature profiles along the test sections. Figure 4(a) is for a fluid inlet velocity of 10.5 feet per second (3.2 m/sec). The open symbols connected by the dashed lines represent the plenum inlet test section data. The solid symbols connected by the solid lines are for the straight inlet test section data. Each pair of curves were generated at a constant value of heat flux which allows the data comparison described hereinafter.

The range of heat fluxes employed in the course of this study produced wall temperatures that were indicative of both nucleate and film boiling. Separation of the data into these different modes of heat transfer is shown by the arrows in figure 4(a). Wall temperatures of approximately 50° R (28 K) are representative of nucleate boiling while transition to film boiling occurs at higher temperatures.

Film boiling. - The film boiling data in figure 4(a) represented by the three sets of curves at heat fluxes of 0.27, 0.60, and 1.06 Btu/(sec)(in.^{2}) (44, 98, and 173 W/cm^2) show a consistent trend just downstream of the inlets. At the first measuring station and for some distance downstream the wall temperature of the plenum test section is higher than the straight inlet test section with the temperature differences a function of heat flux.

The effect of velocity on this data trend is shown in figures 4(b) to (e) which present data at inlet velocities from 15 to 47 feet per second (4.6 to 14.3 m/sec). At a heat flux of 1.07 Btu/(sec)(in.^{2}) (175 W/m^2), the trend is consistent but at lower heat fluxes a reversal occurs in the temperature profiles. This phenomenon is first noted in figure 4(c) at a heat flux of 0.27 Btu/(sec)(in.^{2}) (44 W/m^2) for an inlet velocity of 26 feet per second (7.9 m/sec) which shows the plenum test section, just downstream of the inlet, now operating at a lower temperature than the straight inlet test section. On the succeeding plots (figs. 4(d) to (f)), the temperature difference increases with velocity. In figure 4(f) this data trend is noted up to a heat flux of 0.61 Btu/(sec)(in.^{2}) (100 W/m^2).

In general, inlet hydrodynamics influenced film boiling for a distance of about 4 to 8 diameters downstream from the inlet. Wall temperature differences ranging from about zero to 100° R (56 K) were observed depending on the heat flux and the fluid velocity. The reversal in temperature profiles described previously can be explained in terms of the stability of the vapor film at the different heat flux levels.

The higher heat fluxes the vapor film is quite stable so that a flow perturbation at the inlet cannot persist for any appreciable length along the tube. The influence that is noted just downstream of the inlet is caused by fluid acceleration from the plenum through the sharp edge inlet resulting in a vena contracta type of flow separation. The wall region influenced by this vena contracta is subject to relatively stagnant fluid that causes a degradation in heat transfer.

At lower heat fluxes and increased fluid velocities the reversal in temperature profile can be explained in terms of the unstable nature of the vapor film at these heat flux levels and flow conditions. In this case, the magnitude of the flow perturbation at the inlet of the plenum test section is sufficient to drive the front end of the test section into transition boiling.

Transition from nucleate to film boiling. - The influence of inlet hydrodynamics on the transition from nucleate to film boiling is shown in figures 4(a) to (f) at a heat flux of 0.06 Btu/(sec)(in.^{2}) (9.8 W/cm^2). In general, the flow perturbation caused by the plenum inlet prevented the establishment of a vapor film for a heat flux that supports film boiling in the straight inlet test section. These data were replotted in figure 5 to more conveniently examine the velocity influence on this transition phenomenon.

Figure 5(a) shows the data comparison at a fluid inlet velocity of 10.5 feet per second (3.2 m/sec). The front half of the plenum test section is in the nucleate boiling regime while the downstream half is operating in transition and film boiling. Under the same test conditions, the straight inlet test section operates completely in the film boiling regime. A temperature difference of about 200° R (111 K) exists over part of the tube that has been wetted by the fluid.

Figure 5(b) shows the effect of an increase in velocity to 26 feet per second (7.9 m/sec) on the temperature profiles. The downstream end of the plenum test section is now in nucleate boiling so that each test section operates in a different boiling regime over its entire length.

As the velocity is increased to 47 feet per second (14.3 m/sec) in figure 5(c), a drop in temperature at the upstream end of the straight inlet test section indicates the start of transition to nucleate boiling. This trend is then completed in figure 5(d) at an inlet velocity of 67 feet per second (20.4 m/sec) which shows both test sections now operating in the nucleate boiling regime.

In summary then, film boiling at comparatively low heat fluxes can be influenced by both the flow perturbation caused by the plenum inlet and the increased convection at

higher inlet velocities. This sensitivity is a result of the low energy nature of the vapor film for heat fluxes at which transition can occur.

Near Critical Heat Transfer

The basic near critical hydrogen heat transfer data for system absolute pressures of 200 and 300 psi (13.8×10^5 and 20.7×10^5 N/m^2) at inlet velocities from about 11 to 68 feet per second (3.4 to 20.7 m/sec) are presented in table II. In general, the wall temperature distributions were dramatically influenced by entrance conditions at higher heat fluxes.

Typical results are presented in figure 6 for test conditions that include an absolute pressure of 300 psi (20.7×10^5 N/m^2), inlet velocity of 32 feet per second (9.8 m/sec), and inlet bulk temperature of 48° R (27 K). The comparative curves at a heat flux of 1.07 Btu/(sec)(in.^{2}) (175 W/cm^2) show the entire plenum inlet test section operating at a significantly lower temperature than the straight inlet test section. At the downstream end, a temperature difference exists of about 140° R (78 K). As the heat flux is reduced this temperature difference decreases until it is on the order of data reproducibility or measurement accuracy.

For this particular set of data only the two pairs of curves at the higher heat fluxes are considered as being significantly influenced by differences in inlet conditions. An examination of the balance of the data in table II will show that the heat flux at which this data separation can be made is a function of fluid inlet velocity.

An attempt to explain the lower wall temperatures throughout the plenum inlet test section may be made with the help of a flow model from reference 1 for near critical heat transfer that describes the system as being composed of packets of high (cold) and low (hot) density fluid. In the straight inlet test section the higher temperature fluid would tend to stratify along the wall while induced turbulence caused by the plenum inlet would tend to break up the fluid into individual packets. An increase in the lateral motion of these individual packets would permit greater penetration of the colder packets to the wall with a subsequent reduction in wall temperature.

What is most surprising, though, is the persistence of the effect of inlet conditions for the entire test section length (x/d = 20). It is possible that the nature of "interfacial" forces between the high and low density packets of fluid allow the motion of these individual packets to be quite sensitive to the turbulence level.

The data in figure 6 at a heat flux of 1.07 Btu/(sec)(in.^{2}) (175 W/cm^2) are presented in figure 7 in terms of local heat transfer coefficients plotted against the x/d ratio along the tube. The heat transfer coefficients decrease downstream of the inlet for both the plenum and straight inlet test sections. The effect of the plenum was to significantly

raise the heat transfer coefficients from the inlet to the exit of the test section. If the test sections had been longer, both curves should eventually have had to converge at some x/d value beyond which the influence of inlet conditions could no longer be felt.

Figure 8 was obtained from the data in figure 7 by ratioing the plenum test section heat transfer coefficients to the straight inlet coefficients and expressing them in terms of a Nusselt number ratio for reference data comparison. The positive slope of a curve connecting these data points appears to be constant with the Nusselt number ratio near the inlet of 1.4 increasing to 1.9 at the exit. It is quite significant that this ratio is still increasing out to an x/d of 18.5. If the test section had been longer, the effect of inlet conditions as represented by the Nusselt number ratio would be expected to reach a maximum at some finite x/d ratio and then drop off to unity.

This enhancement and maximization in heat transfer downstream of a flow perturbation has been described in reference 6 for a system that used orifices at the inlet of a test section to induce flow separation. The data presented therein were limited to forced convection heat transfer at low pressure over a range of bulk Reynolds numbers with water as the working fluid. Although these test conditions are quite different, a comparison was made with the present near critical hydrogen data and presented in figure 9.

The reference 6 water data at a bulk Reynolds number of 100 000 is represented by the dashed curve in figure 9. It was calculated from the data in figure 5 of reference 6 that represents orifice and straight inter conditions. A Nusselt number ratio that conforms to the definition used in the present study was obtained by dividing the orifice inlet data by the straight inlet data. Results of this calculation show that the Nusselt number ratio maximizes to a value of 2.9 at an x/d ratio of about 2 and drops off to unity in the downstream direction at an x/d ratio of about 12. The authors of reference 6 suggest that the location of this maximum coincides with the point of flow re-attachment with the enhancement in heat transfer essentially being due to increased turbulence in the separated region that decreases downstream of the re-attachment position.

The solid line in figure 9 represents the present near critical hydrogen data replotted from figure 8 for an average bulk Reynolds number of 830 000. This curve indicates an enhancement in heat transfer induced by the plenum inlet but does not show any tendency to maximize within the bounds of the test section. This order of magnitude difference in the position of maximum heat transfer cannot be explained by inlet geometry or test differences. It is, therefore, suggested that these results may be tied to fluid property differences that are unique for the thermodynamic regimes within which these systems operate.

Correlation of Near Critical Data

The near critical data found to be influenced by hydrodynamic entrance conditions lie in a range of practical interest with test conditions comparable to a coolant channel inlet of a regeneratively cooled rocket engine. This similarity justified an attempt at correlating these results even with the quite limited set of data obtained in this investigation. The procedure was to modify an existing equation from the published literature in some manner to comprehend differences in inlet hydrodynamic conditions. The following equation based on fluid bulk properties was obtained from reference 3:

$$Nu_b = 0.023\ Re_b^{0.8} Pr_b^{0.4} \left(\frac{T_w}{T_b}\right)^{\{-0.57+[1.59/(x/d)]\}} \tag{7}$$

Figure 10 presents the attempted correlation of straight inlet data with equation (7) represented by the solid line. Although trends for individual runs did not always follow the slope of this line, most of the data falls within a ±30 percent scatter. It should be understood that the correlation itself is quite limited because of certain restrictions placed on the data. The thermocouples closest to the electrodes at the inlet and exit end of the test section were not included since they are the most likely to be subject to axial conduction. The data runs that were correlatable are noted in figure 10 with the balance of the data falling into two categories. Data run with wall temperatures below 65° R (36 K) were not included because the small temperature differences between the wall and bulk fluid coupled with thermocouple accuracy made the calculation of heat transfer coefficients quite inaccurate. Two runs (256 and 260) at higher heat fluxes were eliminated because equation (7) could not comprehend the axial variation of fluid properties through the transposed critical point with any degree of accuracy.

Accepting figure 10 as the representation of a reasonable correlation for this type of heat transfer data the next step was to apply equation (7) to the plenum inlet data. In this case, a further complexity was anticipated because at low heat fluxes and/or high Reynolds number the effect of inlet hydrodynamics was not measureable. A criterion for separating the data was established by data comparison at a specific wall temperature measuring location near the downstream end of the test section. An example of these data comparisons is presented in figure 11 which shows the manner in which inlet hydrodynamic conditions influence the wall temperature at an x/d location of 15.3 for three different inlet fluid velocities.

In figure 11(a), the data obtained at an inlet velocity of 15 feet per second (4.6 m/sec) (Re_{in} = 207 000) show the curves to be coincident at a heat flux level of ≈0.06 Btu/(sec)(in.^{2}) (9.8 W/cm^2). At higher heat fluxes the curves diverge with the plenum

inlet test section operating at a significantly lower temperature than that of the straight inlet test section. The succeeding figures (figs. 11(b) and (c)) show that the heat flux at which the curves start to diverge is a function of inlet velocity.

The data from table II were treated in this manner and the results plotted in figure 12 in terms of heat flux at the point of divergence as a function of Reynolds number. The locus of these divergence points form a band that separates the graph into two regions. Test conditions identified by heat flux and Reynolds number that fall within the band itself and in the region to the right of it are not significantly or measurably influenced by differences in hydrodynamic inlet conditions. While test conditions in the region left of the band, can be quite sensitive to inlet hydrodynamics. The particular data runs that fall into this category are listed in figure 13 which presents the correlation of data found sensitive to inlet conditions. The dashed line of figure 13 represents equation (7) that only includes fully developed inlet flow. As expected, the data fall above this line indicating higher heat transfer rates. An effective correlation of the data was then obtained by changing the constant in equation (7) from 0.023 to 0.036. The solid line in the plot represents the modified equation with the amount of data scatter comparable to the straight inlet data correlation of figure 10. The change in equation constant represents an average increase of about 57 percent in the heat transfer rate.

SUMMARY OF RESULTS

An experimental investigation was made to determine the influence of hydrodynamic entrance conditions on hydrogen heat transfer in both the boiling and near critical thermodynamic regimes. Comparisons were made with data from two electrically (resistance) heated test sections having identical dimensions but different inlet geometries that produced fully developed flow or undeveloped flow at the start of the heating lengths.

The range of data includes boiling at absolute pressures of 35 to 100 psi (2.4×10^5 to 6.9×10^5 N/m^2) and near critical heat transfer at absolute pressures of 200 and 300 psi (13.8×10^5 and 20.7×10^5 N/m^2), inlet velocities from 11 to 68 feet per second (3.4 to 20.7 m/sec), heat fluxes from 0.06 to 1.10 Btu/(sec)(in.^{2}) (9.8 to 180 W/cm^2), and inlet bulk temperatures between 43° and 48° R (24 and 27 K).

The following results were obtained for boiling while operating the test sections under identical test conditions:

1. Film boiling heat transfer was influenced by inlet hydrodynamics for a distance of 4 to 8 diameters downstream from the inlet as evidenced by wall temperature differences ranging from zero to about 100° R (56 K) depending on the heat flux level and fluid velocity.

2. At higher heat fluxes, the plenum test section wall temperatures were greater than the straight inlet test section with the temperature difference a function of heat flux.

Explanations were made in terms of flow separation resulting in relatively stagnant fluid along the wall near the inlet.

3. At lower heat fluxes and increased velocities a reversal in the data trend was noted with the inlet end of the plenum test section lower in temperature than the straight inlet test section. Explanations were made in terms of the low energy nature of the vapor film at these heat flux levels.

4. The transition from nucleate to film boiling was influenced by inlet hydrodynamics over the length of the test section. The flow perturbation caused by the plenum inlet prevented the establishment of a vapor film at heat fluxes that supported film boiling in the straight inlet test section with temperature differences existing of as much as 200° R (111 K).

The following results were obtained for near critical heat transfer:

1. The near critical heat transfer data showed that in comparison to fully developed inlet conditions the plenum inlet could raise the heat transfer rates over the entire test section length with differences in the data increasing with heat flux and decreasing with Reynolds number.

2. At higher heat fluxes the wall temperatures on the plenum test section were significantly lower than on the straight inlet test section. This temperature difference decreased as the heat flux was reduced until it was not measureable.

3. Explanation for the higher plenum inlet heat transfer rates were made in terms of induced turbulence on a model for heat and mass transfer that is unique for near critical fluids.

4. Comparative trends were made with published forced convection, subcritical water data from a rig with a flow configuration that induced inlet turbulence. The most significant difference was that the enhanced heat transfer caused by the inlet geometry on the forced convection system maximized at an x/d of 2 while it was still increasing at an x/d of 18.5 for the near critical system.

5. The straight inlet data were correlated directly with equation (7) obtained from reference 3 which comprehends only fully developed flow at the inlet to the test section. The plenum inlet data that were found sensitive to hydrodynamic entrance conditions were correlated by a modification of equation (7) that yields an average increase of about 57 percent in the heat transfer rates.

Lewis Research Center,
National Aeronautics and Space Administration,
Cleveland, Ohio, October 29, 1970,
129-01.

APPENDIX - SYMBOLS

d	diameter
H	enthalpy
h	heat transfer coefficient
K	constant in eq. (2)
k	thermal conductivity
L	length of test section
Nu	Nusselt number
Pr	Prandtl number
p	pressure
Q	heat flow
q	heat flux
Re	Reynolds number
r	radius of tube
T	temperature
V	velocity
x	local position measured from inlet
μ	absolute viscosity
ρ	density
$\dot{\omega}$	flow rate

Subscripts:

b	bulk
d	fully developed flow inlet
i	inside surface
in	inlet
m	metal
out	outlet
o	outside surface
p	plenum inlet
sat	saturated
s	straight inlet
u	undeveloped flow inlet
w	wall
x	local position measured from inlet

REFERENCES

1. Hendricks, R. C.; Graham, R. W.; Hsu, Y. Y.; and Medeiros, A. A.: Correlation of Hydrogen Heat Transfer in Boiling and Supercritical Pressure States. ARS J., vol. 32, no. 2, Feb. 1962, pp. 244-252.

2. Hess, H. L.; and Kunz, H. R.: A Study of Forced Convection Heat Transfer to Supercritical Hydrogen. J. Heat Transfer, vol. 87, no. 1, Feb. 1965, pp. 41-48.

3. Taylor, Maynard F.: Correlation of Local Heat Transfer Coefficients for Single Phase Turbulent Flow of Hydrogen in Tubes with Temperature Ratios to 23. NASA TN D-4332, 1968.

4. Hendricks, R. C.; and Simon, F. F.: Heat Transfer to Hydrogen Flowing in a Curved Tube. Multi-Phase Flow Symposium. Norman J. Lipstein, ed., ASME, 1963, pp. 90-93.

5. Anon.: Heat Transfer to Cryogenic Hydrogen Flowing Turbulently in Straight and Curved Tubes at High Heat Fluxes. NASA CR-678, 1967.

6. Krall, K. M.; and Sparrow, E. M.: Turbulent Heat Transfer in the Separated, Reattached, and Redevelopment Regions of a Circular Tube. J. Heat Transfer, vol. 88, no. 1, Feb. 1966, pp. 131-136.

7. Williams, P. S.; and Knudsen, J. G.: Local Rates of Heat Transfer and Pressure Losses in the Vicinity of Annular Orifices. Can. J. Chem. Eng., vol. 41, no. 2, Apr. 1963, pp. 56-61.

8. McAdams, William H.: Heat Transmission. Third ed., McGraw-Hill Book Co., Inc., p. 19.

9. Harry, David P., III: Formulation and Digital Coding of Approximate Hydrogen Properties for Application to Heat-Transfer and Fluid-Flow Computations. NASA TN D-1664, 1963.

TABLE I. - SUBCRITICAL (BOILING) HYDROGEN DATA

[Inconel X tube: inside diameter, 0.311 in. (0.790 cm); outside diameter, 0.331 in. (0.840 cm).]

(a-1) Straight inlet; U. S. customary units

Run	Inlet pressure, p_{in}, lb/in.^{2}	Outlet pressure, p_{out}, lb/in.^{2}	Flow rate, ω, lb/sec	Inlet velocity, V_{in}, ft/sec	Inlet bulk temperature, $T_{b,in}$, ^oR	Outlet bulk temperature, $T_{b,out}$, ^oR	Saturation temperature, T_{sat}, ^oR	Heat flux, q, Btu/(sec)(in.^{2})	Local fluid side wall temperature[a], $T_{w,i}$, ^oR at x/d values of					
									2.4	5.7	8.9	12.1	15.3	18.5
171	33	32	0.025	11.6	42	42	42	0.06	205	221	231	236	238	242
172	39	38	.022	10.2	43	43	43	.27	508	531	568	558	637	685
173	38	36	.023	10.6	43	93	43	.61	1017	1046	1123	1193	1196	1163
175	36	35	.033	15.4	43	43	43	.06	213	218	222	221	221	223
176	35	33	.034	15.5	42	42	42	.27	485	485	499	500	509	528
180	40	39	.059	27.1	43	43	43	.06	196	207	211	208	206	205
181	42	39	.058	27.0	44	43	44	.27	415	403	405	399	387	392
183	43	34	.057	26.6	43	42	43	1.10	922	855	796	805	802	865
185	38	36	.072	33.4	43	42	43	.06	185	198	204	201	200	199
186	38	33	.073	30.2	43	42	43	.27	394	389	390	379	376	380
187	42	34	.072	33.4	43	42	43	.62	453	508	509	524	524	542
188	51	41	.071	33.7	45	43	45	1.09	859	771	679	714	724	775
190	40	37	.102	47.1	43	42	43	.06	178	200	212	206	203	203
191	41	34	.103	47.8	43	42	43	.27	363	348	344	335	321	320
192	50	41	.102	47.3	43	43	45	.62	480	487	504	509	488	494
193	61	49	.102	47.2	44	45	46	1.11	826	770	596	699	674	699
195	49	48	.022	10.7	45	45	45	.06	260	256	253	249	246	246
196	49	47	.022	10.3	45	45	45	.27	507	485	488	489	480	497
197	47	45	.022	10.6	45	44	45	.61	820	770	778	800	758	851
198	48	41	.022	10.5	44	89	44	1.08	1161	1125	1145	1197	1214	---
200	47	46	.032	15.2	45	45	45	.07	262	257	249	242	236	237
201	50	48	.030	14.4	45	45	↓	.27	493	427	421	427	426	440
203	49	43	.032	15.1	45	49	↓	1.09	979	848	876	952	999	1098
205	48	47	.056	26.2	44	45	↓	.06	228	239	244	238	234	234
206	49	47	.056	26.0	44	45	↓	.27	438	415	413	408	397	404
208	52	44	.056	26.0	44	44	45	1.09	892	815	765	795	800	856
210	52	50	.071	33.0	↓	45	46	.06	192	215	234	234	234	234
211	47	43	.072	33.4	↓	44	45	.27	412	395	390	382	370	374
212	51	45	.072	33.3	↓	44	45	.61	478	491	512	526	535	557
213	51	41	.072	33.4	↓	43	45	1.09	879	779	---	711	720	768
215	49	47	.102	46.8	43	44	45	.07	147	176	202	218	229	234
216	48	43	.102	46.9	↓	44	45	.27	394	385	385	375	360	362
217	50	41	.103	47.4	↓	43	45	.61	481	488	504	511	490	495
218	60	48	.102	46.9	↓	45	46	1.10	824	771	720	700	676	697
219	55	51	.145	66.2	42	43	46	.06	52	50	50	46	47	52
220	55	50	.146	66.6	42	45	46	.27	350	390	402	388	375	377
221	58	48	.145	66.4	43	45	46	.61	458	490	509	519	499	492
223	96	96	.024	11.4	46	50	52	.06	251	286	303	306	304	304
224	99	99	.022	10.4	46	52	52	.27	503	505	497	498	491	500
225	100	98	.023	10.8	46	52	52	.61	859	778	752	752	740	764
226	97	94	.023	11.0	46	71	52	1.10	1206	1054	976	991	1022	1103
228	100	100	.031	14.7	↓	49	↓	.06	222	261	287	289	299	298
229	96	95	.033	15.4	↓	52	↓	.28	490	478	468	469	463	472
230	99	97	.031	14.9	↓	52	↓	.62	794	755	722	712	695	708
231	97	95	.032	15.4	↓	55	↓	1.10	1086	1002	948	956	963	1028

[a]Average value - two thermocouples at each location.

TABLE I. - Continued. SUBCRITICAL (BOILING) HYDROGEN DATA

[Inconel X tube: inside diameter, 0.311 in. (0.790 cm); outisde diameter, 0.331 in. (0.840 cm).]

(a-2) Straight inlet; SI units

Run	Inlet pressure, p_{in}, N/m^2	Outlet pressure, p_{out}, N/m^2	Flow rate, $\dot{\omega}$, kg/sec	Inlet velocity, V_{in}, m/sec	Inlet bulk temperature, $T_{b,in}$, K	Outlet bulk temperature, $T_{b,out}$, K	Saturation temperature, T_{sat}, K	Heat flux, q, W/cm^2	Local fluid side wall temperature[a], $T_{w,i}$, K at x/d values of					
									2.4	5.7	8.9	12.1	15.3	18.5
171	2.3×10^5	2.2×10^5	0.011	3.54	23	23	23	9.8	114	123	128	131	132	134
172	2.7	2.6	.010	3.11	24	24	24	44.0	282	295	316	310	354	380
173	2.6	2.5	.010	3.23	24	52	24	100.0	564	580	625	663	665	647
175	2.5	2.4	.015	4.70	24	24	24	9.8	118	121	123	123	123	124
176	2.4	2.3	.015	4.73	23	23	23	44.0	269	269	276	278	282	293
180	2.8×10^5	2.7×10^5	.027	8.26	24	24	24	9.8	109	115	117	116	115	114
181	2.9	2.7	.026	8.25	↓	24	↓	44.0	231	224	225	221	215	218
183	3.0	2.3	.026	8.11	↓	23	↓	180.0	512	475	443	447	445	480
185	2.6	2.5	.033	10.2	↓	23	↓	9.8	103	110	113	112	111	110
186	2.6	2.3	.033	9.21	↓	23	↓	44.0	219	216	216	210	209	211
187	2.9×10^5	2.3×10^5	.033	10.2	24	23	24	101.0	252	282	282	290	290	301
188	3.5	2.8	.032	10.3	25	24	25	178.0	477	429	377	396	402	430
190	2.8	2.6	.046	14.4	24	23	24	9.8	99	111	118	115	113	113
191	2.8	2.3	.047	14.6	24	23	24	44.0	202	193	191	186	178	178
192	3.4	2.8	.046	14.4	24	24	25	101.0	266	271	280	282	271	274
193	4.2×10^5	3.4×10^5	.046	14.4	24	25	26	181.0	460	428	332	388	374	388
195	3.4	3.3	.010	3.26	25	25	25	9.8	145	142	141	138	137	137
196	3.4	3.2	.010	3.14	25	25	25	44.0	282	270	271	272	267	276
197	3.2	3.1	.010	3.24	25	24	25	100.0	455	427	432	445	421	473
198	3.3	2.8	.010	3.20	24	50	24	177.0	645	625	636	664	674	---
200	3.2×10^5	3.2×10^5	.016	4.64	25	25	25	11.0	146	143	138	135	131	132
201	3.5	3.3	.014	4.40	25	25	↓	44.0	274	237	234	237	237	244
203	3.4	3.0	.016	4.61	25	27	↓	178.0	544	471	487	529	555	560
205	3.3	3.2	.025	8.00	24	25	↓	9.8	127	133	136	132	130	130
206	3.4	3.2	.025	7.94	24	25	↓	44.0	244	230	229	227	220	224
208	3.6×10^5	3.0×10^5	.025	7.94	24	24	25	178.0	495	452	425	442	445	476
210	3.6	3.5	.032	10.1	↓	25	26	9.8	107	119	130	130	130	130
211	3.2	3.0	.033	10.2	↓	24	25	44.0	229	219	216	212	206	208
212	3.5	3.1	.033	10.2	↓	24	25	100.0	266	273	284	292	297	310
213	3.5	2.8	.033	10.2	↓	24	25	178.0	487	432	---	396	400	426
215	3.4×10^5	3.2×10^5	.046	14.3	24	24	25	11.0	82	98	112	121	127	130
216	3.3	3.0	.046	14.3	24	24	25	44.0	219	214	214	208	200	201
217	3.5	2.8	.047	14.4	24	24	25	100.0	268	271	280	284	272	275
218	4.1	3.3	.046	14.3	24	25	26	180.0	457	429	400	389	376	388
219	3.8	3.5	.066	20.2	23	24	26	9.8	29	28	28	26	26	29
220	3.8×10^5	3.4×10^5	.066	20.3	23	25	26	44.0	195	216	223	216	208	204
221	4.0	3.3	.066	20.2	24	25	26	100.0	254	272	282	288	277	273
223	6.6	6.6	.011	3.48	26	28	29	9.8	140	159	168	170	169	169
224	6.8	6.8	.010	3.18	26	29	29	44.0	279	280	276	276	273	278
225	6.9	6.8	.010	3.30	26	29	29	100.0	476	432	418	418	411	424
226	6.7×10^5	6.5×10^5	.010	3.36	26	39	29	180.0	670	586	542	550	569	614
228	6.9	6.9	.014	4.49	↓	27	↓	9.8	123	145	159	161	166	166
229	6.6	6.5	.015	4.70	↓	29	↓	46.0	272	266	260	260	257	262
230	6.8	6.7	.014	4.55	↓	29	↓	101.0	441	419	401	396	386	393
231	6.7	6.5	.015	4.70	↓	31	↓	180.0	604	557	526	531	535	570

[a]Average value - two thermocouples at each location.

TABLE I. - Continued. SUBCRITICAL (BOILING) HYDROGEN DATA

[Inconel X tube: inside diameter, 0.311 in. (0.790 cm); outside diameter, 0.331 in. (0.840 cm).]

(b-1) *Plenum inlet; U. S. customary units*

Run	Inlet pressure, p_{in}, lb/in.^{2}	Outlet pressure, p_{out}, lb/in.^{2}	Flow rate, ω, lb/sec	Inlet velocity, V_{in}, ft/sec	Inlet bulk temperature, $T_{b,in}$, ^oR	Outlet bulk temperature, $T_{b,out}$, ^oR	Saturation temperature, T_{sat}, ^oR	Heat flux, q, Btu/(sec)(in.^{2})	Local fluid side wall temperature[a], $T_{w,i}$, ^oR at x/d values of					
									2.4	5.7	8.9	12.1	15.3	18.5
65	43	43	0.022	10.3	44	44	44	0.06	48	47	247	241	236	237
67	35	33	.022	10.3	42	96	42	.58	1116	1039	1097	1145	1148	1108
69	36	36	.031	14.1	43	43	43	.06	51	46	114	230	203	222
70	31	31	.031	14.3	42	41	42	.27	525	489	488	499	495	494
71	32	29	.031	14.2	42	51	41	.58	879	843	826	830	817	804
72	39	34	.033	15.1	43	70	43	1.07	1157	1096	1005	1014	1033	1064
74	36	34	.056	26.0	42	42	42	.06	49	46	49	54	48	186
75	36	33	.056	26.0	42	42	42	.27	467	422	409	412	401	397
77	39	31	.055	25.4	43	41	43	1.10	976	912	813	803	813	835
79	37	35	.073	33.6	43	42	43	.06	51	44	51	53	44	50
80	41	37	.072	33.4	43	43	43	.27	365	388	372	367	353	347
82	50	40	.073	33.5	↓	43	45	1.07	909	812	728	717	720	730
84	39	34	.102	46.8	↓	42	43	.06	53	47	49	53	45	49
85	46	40	.102	47.0	↓	43	44	.28	305	373	378	376	358	348
86	51	41	.102	46.9	↓	43	45	.61	485	542	525	526	498	485
87	60	50	.101	46.5	43	45	46	1.07	856	816	743	700	668	663
89	56	56	.019	9.1	46	46	46	.06	49	47	51	126	226	237
90	47	47	.022	10.4	45	45	45	.27	534	514	498	499	498	493
91	49	47	.021	9.8	45	45	45	.60	870	791	760	779	788	801
92	48	45	.022	10.2	45	91	45	1.04	1200	1127	1081	1140	1181	1223
94	45	45	.030	14.3	45	45	45	.06	50	47	51	53	46	50
95	46	45	.031	14.7	45	44	↓	.27	510	464	439	434	424	421
97	50	46	.031	14.7	45	49	↓	1.04	1070	924	865	911	952	994
99	48	47	.056	26.0	44	45	↓	.06	55	50	53	58	49	53
100	48	46	.055	25.8	44	45	↓	.26	405	432	412	405	387	380
102	48	41	.055	25.7	44	44	44	1.06	971	881	795	783	784	796
104	48	46	.073	34.0	43	44	45	.06	49	45	49	52	44	48
105	49	45	.072	33.5	43	45	45	.27	355	417	411	407	387	378
106	50	44	.071	33.1	44	44	45	.60	485	516	558	547	534	530
107	50	39	.072	33.5	44	43	44	1.05	920	795	714	703	707	715
109	51	48	.102	46.8	43	44	45	.06	49	47	50	55	45	50
110	49	43	.102	46.9	43	44	45	.27	286	372	390	393	376	365
113	58	46	.099	45.0	43	45	46	1.05	871	834	751	709	668	661
117	54	43	.141	67.2	45	44	45	.06	54	51	52	57	50	55
118	58	47	.141	68.2	46	45	46	.28	232	307	337	352	335	326
119	67	54	.141	68.1	47	46	47	.62	408	484	507	520	500	479
122	95	94	.023	11.7	51	52	51	.06	60	233	283	303	298	296
123	97	96	.022	11.1	50	52	52	.28	500	530	539	533	520	512
124	95	95	.022	11.1	50	52	52	.62	---	786	755	716	702	736
125	99	98	.022	10.9	50	92	52	1.10	1238	1098	985	1014	1091	1167
126	95	94	.031	14.9	48	51	51	.07	60	59	64	221	269	285
127	94	93	.031	15.0	48	52	51	.27	468	529	541	544	526	510
129	98	96	.032	15.6	48	61	52	1.09	---	1031	914	867	911	988

[a]Average value - two thermocouples at each location.

TABLE I. - Concluded. SUBCRITICAL (BOILING) HYDROGEN DATA

[Inconel X tube: inside diameter, 0.311 in. (0.790 cm); outside diameter, 0.331 in. (0.840 cm).]

(b-2) Plenum inlet; SI units

Run	Inlet pressure, p_{in}, N/m^2	Outlet pressure, p_{out}, N/m^2	Flow rate, $\dot{\omega}$, kg/sec	Inlet velocity, V_{in}, m/sec	Inlet bulk temperature, $T_{b,in}$, K	Outlet bulk temperature, $T_{b,out}$, K	Saturation temperature, T_{sat}, K	Heat flux, q, W/cm^2	Local fluid side wall temperature[a], $T_{w,i}$, K at x/d values of					
									2.4	5.7	8.9	12.1	15.3	18.5
65	3.0×10^5	3.0×10^5	0.010	3.12	24	24	24	9.8	27	26	137	134	131	132
67	2.4	2.3	.010	3.12	23	53	23	95.0	620	576	609	635	637	615
69	2.5	2.5	.014	4.30	24	24	24	9.8	28	26	63	128	113	123
70	2.1	2.1	.014	4.36	23	23	23	44.0	292	272	271	277	275	274
71	2.2	2.2	.014	4.33	23	28	23	95.0	488	469	459	461	454	447
72	2.7×10^5	2.3×10^5	.015	4.60	24	39	24	175.0	642	610	560	564	574	592
74	2.4	2.3	.025	7.93	23	23	23	9.8	27	26	27	30	27	103
75	2.4	2.3	.026	7.93	23	23	23	44.0	260	234	227	228	223	220
77	2.7	2.1	.025	7.75	24	23	24	180.0	542	507	452	445	452	464
79	2.6	2.4	.033	10.3	24	23	24	9.8	28	24	28	29	24	28
80	2.8×10^5	2.6×10^5	.033	10.2	24	24	24	44.0	202	215	206	204	202	193
82	3.4	2.8	.033	10.2	↓	24	25	175.0	504	450	404	398	400	405
84	2.7	2.3	.046	14.3		23	24	9.8	29	26	27	29	25	27
85	3.2	2.8	.046	14.3		24	24	46.0	169	207	210	208	199	193
86	3.5	2.8	.046	14.3		24	25	100.0	269	301	292	292	276	269
87	4.1×10^5	2.5×10^5	.046	14.2	24	25	26	175.0	475	453	412	388	371	368
89	3.9	3.9	.009	2.78	26	26	26	9.8	27	26	28	70	125	132
90	3.2	3.2	.010	3.17	25	25	25	44.0	296	286	276	277	276	274
91	3.4	3.2	.010	2.98	25	25	25	98.0	483	440	422	432	437	445
92	3.3	3.1	.010	3.11	25	51	25	170.0	665	625	600	632	656	678
94	3.1×10^5	3.1×10^5	.014	4.36	25	25	25	9.8	28	26	28	29	26	28
95	3.2	3.1	.014	4.48	25	24	↓	44.0	283	257	244	241	235	234
97	3.4	3.2	.014	4.49	25	27		170.0	595	513	480	506	529	552
99	3.3	3.2	.025	7.93	24	25		9.8	31	28	29	32	27	29
100	3.3	3.2	.025	7.87	24	25		43.0	225	240	229	225	215	211
102	3.3×10^5	2.8×10^5	.025	7.84	24	24	24	173.0	540	490	442	435	435	442
104	3.3	3.2	.033	10.4	↓	24	25	9.8	27	25	27	29	24	27
105	3.4	3.1	.033	10.2		25	25	44.0	197	232	228	226	215	210
106	3.5	3.0	.032	10.1		24	25	98.0	269	287	310	304	296	294
107	3.5	2.7	.033	10.2		24	24	172.0	511	441	396	390	393	397
109	3.5×10^5	3.3×10^5	.046	14.3	24	24	25	9.8	27	26	28	31	25	28
110	3.4	3.0	.046	14.3	24	24	25	44.0	159	206	216	218	209	203
113	4.0	3.2	.045	13.7	24	25	26	172.0	484	463	417	394	371	368
117	3.7	3.0	.064	20.5	25	24	25	9.8	30	28	29	32	28	31
118	4.0	3.2	.064	20.8	26	25	26	46.0	129	171	187	195	186	181
119	4.6×10^5	3.7×10^5	.064	20.8	26	26	26	101.0	227	269	281	289	278	266
122	6.6	6.5	.010	3.57	28	29	28	9.8	33	129	157	168	165	164
123	6.7	6.6	.010	3.38	28	29	29	46.0	278	294	299	296	289	284
124	6.6	6.6	.010	3.38	28	29	29	101.0	---	437	419	398	390	410
125	6.8	6.8	.010	3.32	28	51	29	180.0	686	610	547	564	606	647
126	6.6×10^5	6.5×10^5	.014	4.55	27	28	28	11.0	33	33	36	117	149	158
127	6.5	6.4	.014	4.57	27	29	28	44.0	260	294	301	302	292	283
129	6.8	6.6	.015	4.76	27	34	29	178.0	---	574	507	482	506	549

[a]Average value - two thermocouples at each location.

TABLE II. - NEAR CRITICAL HYDROGEN DATA

[Inconel X tube: inside diameter, 0.311 in. (0.790 cm); outside diameter, 0.331 in. (0.840 cm).]

(a-1) Straight inlet; U. S. customary units

Run	Inlet pressure, p_{in}, lb/in.^{2}	Outlet pressure, p_{out}, lb/in.^{2}	Flow rate, $\dot{\omega}$, lb/sec	Inlet velocity, V_{in}, ft/sec	Inlet bulk temperature, $T_{b,in}$, ^oR	Outlet bulk temperature, $T_{b,out}$, ^oR	Heat flux, q, $\frac{Btu}{(sec)(in.^2)}$	x/d	Bulk temperature, T_b, ^oR	Inside surface wall temperature, $T_{w,i}$, ^oR	Bulk velocity, V_b, ft/sec	Heat transfer coefficient, h, $\frac{Btu}{(sec)(in.^2)(^oR)}$	Bulk Reynolds number, Re_b	Bulk Prandtl number, Pr_b	Bulk Nusselt number, Nu_b
254	196	196	0.022	10.6	48	53	0.06	2.4	49	81	10.7	1.89×10^{-3}	1.67×10^5	1.24	388
								5.7	48	88	10.8	1.59	1.73	1.25	327
								8.9	50	87	10.9	1.66	1.79	1.26	345
								12.1	51	85	11.1	1.80	1.84	1.27	374
								15.3	52	88	11.2	1.68	1.90	1.29	353
								18.5	52	92	11.4	1.54	1.97	1.31	325
255	196	196	0.023	10.6	47	59	0.27	2.4	50	209	11.0	1.66×10^{-3}	1.77×10^5	1.25	343
								5.7	53	175	11.6	2.16	2.03	1.32	458
								8.9	55	177	12.4	2.17	2.35	1.46	474
								12.1	57	195	13.3	1.92	2.73	1.70	435
								15.3	58	253	14.4	1.35	3.18	2.21	321
								18.5	59	384	15.8	.82	3.70	3.56	204
256	196	196	0.021	10.5	50	89	0.99	2.4	57	335	12.7	3.55×10^{-3}	2.62×10^5	1.73	807
								5.7	59	371	15.0	3.17	3.50	3.50	791
								8.9	61	409	31.4	2.83	6.41	2.71	967
								12.1	66	492	49.0	2.32	6.99	.87	895
								15.3	76	519	68.8	2.23	6.71	.65	930
								18.5	90	688	89.1	1.65	6.13	.61	699
258	194	194	0.033	15.0	46	50	0.06	2.4	46	64	15.2	3.34×10^{-3}	2.25×10^5	1.22	676
								5.7	47	69	15.3	2.66	2.30	1.22	541
								8.9	48	63	15.4	3.79	2.35	1.22	772
								12.1	48	66	15.5	3.27	2.40	1.23	668
								15.3	49	66	15.7	3.37	2.45	1.24	691
								18.5	49	71	15.8	2.68	2.50	1.24	551
259	199	199	0.031	14.2	46	57	0.27	2.4	48	170	14.6	2.20×10^{-3}	2.25×10^5	1.23	449
								5.7	50	196	15.1	1.84	2.49	1.26	383
								8.9	53	203	15.8	1.79	2.76	1.32	378
								12.1	55	209	16.5	1.74	3.08	1.41	376
								15.3	56	248	17.4	1.40	3.43	1.55	311
								18.5	57	273	18.4	1.25	3.84	1.78	285

260	200	199	0.032	15.1	47	67	1.01	2.4	58	317	16.9	3.82×10^{-3}	3.01×10^{5}	1.34	814
								5.7	58	355	20.4	3.40	4.46	2.07	799
								8.9	60	380	26.8	3.15	6.59	6.72	865
								12.1	60	435	37.5	2.69	8.65	9.77	855
								15.3	62	493	52.3	2.34	9.97	1.78	817
								18.5	66	576	70.2	1.97	10.48	.92	748
262	197	197	0.057	25.9	44	47	0.06	2.4	44	59	25.9	4.05×10^{-3}	3.64×10^{5}	1.21	811
								5.7	45	61	26.0	3.64	3.69	↓	730
								8.9	45	58	26.1	4.58	3.73		919
								12.1	45	56	26.2	5.58	3.78		1123
								15.3	46	59	26.3	4.47	3.83	1.22	901
								18.5	46	62	26.4	3.73	3.87	1.22	752
263	204	204	0.054	24.5	45	54	0.27	2.4	46	102	25.0	4.82×10^{-3}	3.68×10^{5}	1.22	974
								5.7	48	110	25.5	4.32	3.90	1.22	881
								8.9	49	115	26.1	4.09	4.13	1.24	841
								12.1	51	119	26.6	3.93	4.38	1.26	816
								15.3	52	122	27.3	3.84	4.64	1.29	805
								18.5	53	148	27.9	2.83	4.93	1.33	601
264	196	195	0.056	25.6	45	58	0.61	2.4	48	265	26.6	2.82×10^{-3}	4.06×10^{5}	1.23	574
								5.7	51	267	27.9	2.83	4.61	1.27	589
								8.9	53	320	29.4	2.30	5.26	1.35	490
								12.1	55	331	31.2	2.22	6.02	1.49	489
								15.3	57	386	33.3	1.86	6.92	1.75	424
								18.5	58	420	36.0	1.70	7.97	2.24	403
266	198	197	0.074	33.4	44	46	0.06	2.4	44	56	33.5	5.24×10^{-3}	4.71×10^{5}	1.21	1049
								5.7	45	59	33.6	4.26	4.76	↓	854
								8.9	↓	56	33.7	5.50	4.80		1105
								12.1		55	33.8	6.21	4.85		1248
								15.3		55	34.0	6.38	4.90	1.22	1285
								18.5	46	54	34.0	7.35	4.95	1.22	1481
267	195	194	0.074	33.3	44	51	0.27	2.4	45	97	33.7	5.17×10^{-3}	4.83×10^{5}	1.21	1038
								5.7	46	103	34.2	4.73	5.04	1.22	956
								8.9	47	111	34.7	4.22	5.26	1.22	858
								12.1	48	118	35.3	3.86	5.49	1.23	791
								15.3	49	123	35.8	3.65	5.73	1.25	753
								18.5	50	144	36.4	2.87	5.98	1.26	597
268	196	195	0.073	32.9	44	57	0.61	2.4	46	245	33.7	3.05×10^{-3}	4.95×10^{5}	1.22	616
								5.7	49	299	34.9	2.42	5.46	1.24	497
								8.9	51	285	36.2	2.59	6.02	1.27	540
								12.1	53	296	37.7	2.50	6.66	1.34	530
								15.3	55	406	39.4	1.73	7.38	1.43	375
								18.5	56	402	41.3	1.75	8.20	1.57	390

TABLE II. - Continued. NEAR CRITICAL HYDROGEN DATA

[Inconel X tube: inside diameter, 0.311 in. (0.790 cm); outside diameter, 0.331 in. (0.840 cm).]

(a-1) Concluded. Straight inlet; U. S. customary units

Run	Inlet pressure, p_{in}, lb/in.^{2}	Outlet pressure, p_{out}, lb/in.^{2}	Flow rate, $\dot{\omega}$, lb/sec	Inlet velocity, V_{in}, ft/sec	Inlet bulk temperature, $T_{b,in}$, ^oR	Outlet bulk temperature, $T_{b,out}$, ^oR	Heat flux, q, Btu/(sec)(in.^{2})	x/d	Bulk temperature, T_b, ^oR	Inside surface wall temperature, $T_{w,i}$, ^oR	Bulk velocity, V_b, ft/sec	Heat transfer coefficient, h, Btu/(sec)(in.^{2})(^oR)	Bulk Reynolds number, Re_b	Bulk Prandtl number, Pr_b	Bulk Nusselt number, Nu_b
270	295	295	0.035	16.2	47	50	0.06	2.4	47	63	16.3	3.63×10^{-3}	2.37×10^5	1.21	727
								5.7	48	67	16.4	2.96	2.42	1.21	596
								8.9	48	60	16.5	4.88	2.46	1.21	983
								12.1	49	64	16.6	3.75	2.51	1.22	757
								15.3	49	64	16.8	3.87	2.55	1.22	784
								18.5	50	68	16.9	3.12	2.60	1.22	634
271	294	294	0.030	14.0	48	60	0.27	2.4	50	154	14.5	2.60×10^{-3}	2.24×10^5	1.22	529
								5.7	53	172	15.0	2.27	2.47	1.25	468
								8.9	55	199	15.6	1.88	2.73	1.29	395
								12.1	57	244	16.3	1.45	3.02	1.34	310
								15.3	59	245	17.1	1.45	3.35	1.42	319
								18.5	60	232	18.0	1.57	3.71	1.53	355
272	301	301	0.032	14.6	47	67	0.60	2.4	51	250	15.5	3.04×10^{-3}	2.46×10^5	1.23	622
								5.7	56	244	16.9	3.21	3.04	1.31	683
								8.9	60	291	18.7	2.61	3.77	1.48	583
								12.1	62	294	21.0	2.61	4.67	1.76	620
								15.3	64	316	24.2	2.40	5.67	2.32	615
								18.5	66	348	28.2	2.14	6.67	2.27	592
273	292	292	0.035	16.0	47	72	1.01	2.4	53	311	17.6	3.91×10^{-3}	2.95×10	1.26	812
								5.7	59	314	20.4	3.96	4.10	1.48	882
								8.9	63	341	24.6	3.63	5.66	2.05	894
								12.1	65	394	31.2	3.06	7.37	2.40	853
								15.3	67	409	40.0	2.95	8.69	1.82	898
								18.5	71	484	50.8	2.44	9.45	1.14	783
275	294	293	0.071	32.0	46	48	0.06	2.4	46	57	32.2	5.41×10^{-3}	4.56×10^5	1.21	1078
								5.7	47	59	32.3	4.66	4.60		931
								8.9		58	32.4	5.19	4.65		1037
								12.1		55	32.5	7.31	4.69		1464
								15.3		56	32.6	6.70	4.73		1342
								18.5	48	63	32.7	3.78	4.78		758

276	294	293	0.072	32.4	46	53	0.28	2.4	47	81	32.9	8.12×10^{-3}	4.74×10^{5}	1.21	1625
								5.7	48	89	33.4	6.77	4.95	1.21	1364
								8.9	49	99	33.9	5.57	5.17	1.22	1129
								12.1	51	108	34.5	4.81	5.39	1.22	981
								15.3	52	115	35.0	4.36	5.63	1.23	895
								18.5	53	131	35.6	3.53	5.87	1.25	730
277	293	292	0.073	33.4	46	59	0.61	2.4	48	209	34.2	3.78×10^{-3}	5.05×10^{5}	1.21	761
								5.7	51	225	35.4	3.49	5.54	1.22	712
								8.9	53	238	36.7	3.29	6.07	1.25	681
								12.1	55	256	38.1	3.03	6.66	1.29	638
								15.3	57	266	39.6	2.91	7.32	1.34	625
								18.5	58	303	41.4	2.49	8.05	1.41	546
278	290	289	0.072	33.4	47	63	1.00	2.4	50	298	34.8	4.05×10^{-3}	5.41×10^{5}	1.22	825
								5.7	54	319	36.9	3.79	6.31	1.27	792
								8.9	57	363	39.5	3.28	7.39	1.36	708
								12.1	60	384	42.6	3.10	8.67	1.51	694
								15.3	62	409	46.5	2.89	10.16	1.73	678
								18.5	63	492	51.3	2.34	11.81	2.08	579
280	298	296	0.104	46.1	44	46	0.06	2.4	44	52	46.2	7.49×10^{-3}	6.21×10^{5}	1.21	1478
								5.7	44	56	46.3	5.04	6.25	1.21	997
								8.9	45	54	46.4	6.22	6.29	1.22	1230
								12.1	↓	51	46.5	9.40	6.34	↓	1860
								15.3		52	46.6	8.33	6.38		1650
								18.5		57	46.7	4.95	6.42		982
281	292	291	0.102	45.9	45	50	0.27	2.4	46	77	46.5	8.62×10^{-3}	6.50×10^{5}	1.22	1716
								5.7	47	77	47.0	8.87	6.70	1.21	1773
								8.9	47	77	47.4	9.13	6.90	1.21	1831
								12.1	48	79	47.9	8.78	7.11	1.21	1769
								15.3	49	77	48.4	9.67	7.32	1.22	1955
								18.5	50	84	48.9	7.91	7.54	1.22	1607
282	287	286	0.103	46.3	45	55	0.60	2.4	47	164	47.2	5.06×10^{-3}	6.73×10^{5}	1.21	1013
								5.7	48	192	48.2	4.15	7.19	1.21	836
								8.9	50	230	49.4	3.31	7.66	1.22	674
								12.1	52	210	50.6	3.76	8.17	1.24	774
								15.3	53	197	51.9	4.14	8.71	1.26	862
								18.5	55	227	53.3	3.46	9.30	1.29	727
283	293	291	0.094	42.9	46	60	0.99	2.4	49	308	44.3	3.81×10^{-3}	6.61×10^{5}	1.21	769
								5.7	52	341	46.2	3.42	7.43	1.23	702
								8.9	54	376	48.4	3.08	8.34	1.28	645
								12.1	57	412	50.9	2.79	9.40	1.34	598
								15.3	59	481	53.8	2.34	10.60	1.44	517
								18.5	60	523	57.2	2.14	11.96	1.57	487

TABLE II. - Continued. NEAR CRITICAL HYDROGEN DATA

[Inconel X tube: inside diameter, 0.311 in. (0.790 cm); outside diameter, 0.331 in. (0.840 cm).]

(a-2) Straight inlet, SI units

Run	Inlet pressure, p_{in}, N/m^2	Outlet pressure, p_{out}, N/m^2	Flow rate, $\dot{\omega}$, kg/sec	Inlet velocity, V_{in}, m/sec	Inlet bulk temperature, $T_{b,in}$, K	Outlet bulk temperature, $T_{b,out}$, K	Heat flux, q, W/cm^2	x/d	Bulk temperature, T_b, K	Inside surface wall temperature, $T_{w,i}$, K	Bulk velocity, V_b, m/sec	Heat transfer coefficient, h, $W/(cm^2)(K)$	Bulk Reynolds number, Re_b	Bulk Prandtl number, Pr_b	Bulk Nusselt number, Nu_b
254	13.5×10^5	13.5×10^5	0.010	3.23	27	29	9.8	2.4	27	45	3.26	0.557	1.67×10^5	1.24	388
								5.7	27	49	3.30	.469	1.73	1.25	327
								8.9	28	48	3.32	.489	1.79	1.26	345
								12.1	28	47	3.38	.530	1.84	1.27	374
								15.3	29	49	3.42	.495	1.90	1.29	353
								18.5	29	51	3.48	.454	1.97	1.31	325
255	13.5×10^5	13.5×10^5	0.010	3.23	26	33	44.0	2.4	28	116	3.36	0.490	1.77×10^5	1.25	343
								5.7	29	97	3.54	.636	2.03	1.32	458
								8.9	31	98	3.78	.640	2.35	1.46	474
								12.1	32	108	4.51	.565	2.73	1.70	435
								15.3	32	141	4.40	.398	3.18	2.21	321
								18.5	33	213	4.82	.242	3.70	3.56	204
256	13.5×10^5	13.5×10^5	0.010	3.20	28	49	162.0	2.4	32	186	3.88	1.045	2.62×10^5	1.73	807
								5.7	33	206	4.57	.934	3.50	3.50	791
								8.9	34	227	9.58	.834	6.41	2.71	967
								12.1	37	273	14.90	.683	6.99	.87	895
								15.3	42	288	21.0	.657	6.71	.65	930
								18.5	50	382	27.2	.486	6.13	.61	699
258	13.4×10^5	13.4×10^5	0.015	4.47	26	28	9.8	2.4	26	36	4.64	0.984	2.25×10^5	1.22	676
								5.7	26	38	4.66	.783	2.30	1.22	541
								8.9	27	35	4.69	1.115	2.35	1.22	772
								12.1	↓	37	4.73	.962	2.40	1.23	668
								15.3		37	4.79	.992	2.45	1.24	691
								18.5		39	4.82	.790	2.50	1.24	551
259	13.7×10^5	13.7×10^5	0.014	4.33	26	32	44.0	2.4	27	94	4.45	0.648	2.25×10^5	1.23	449
								5.7	28	109	4.60	.542	2.49	1.26	383
								8.9	29	113	4.82	.527	2.76	1.32	378
								12.1	31	116	5.03	.512	3.08	1.41	376
								15.3	31	138	5.30	.412	3.43	1.55	311
								18.5	32	152	5.60	.368	3.84	1.78	285

260	13.8×10^5	13.7×10^5	0.015	4.60	26	37	165.0	2.4	32	176	5.15	1.125	3.01×10^5	1.34	814
								5.7	32	197	6.22	1.000	4.46	2.07	799
								8.9	33	211	8.17	.926	6.59	16.72	865
								12.1	33	242	10.4	.792	8.65	9.77	855
								15.3	34	274	15.9	.699	9.97	1.78	817
								18.5	37	320	21.4	.580	10.48	.92	748
262	13.6×10^5	13.6×10^5	0.026	7.90	24	26	9.8	2.4	24	33	7.90	1.191	3.64×10^5	1.21	811
								5.7	25	34	7.93	1.070	3.69	↓	730
								8.9	25	32	7.95	1.350	3.73		919
								12.1	25	31	8.00	1.641	3.78		1123
								15.3	26	33	8.02	1.318	3.83	1.22	901
								18.5	26	34	8.05	1.100	3.87	1.22	752
263	14.1×10^5	14.1×10^5	0.025	7.47	25	30	44.0	2.4	26	57	7.63	1.420	3.68×10^5	1.22	974
								5.7	27	61	7.79	1.270	3.90	1.22	881
								8.9	27	64	7.96	1.202	4.13	1.24	841
								12.1	28	66	8.12	1.159	4.38	1.26	816
								15.3	29	68	8.32	1.130	4.64	1.29	805
								18.5	29	82	8.50	.833	4.93	1.33	601
264	13.5×10^5	13.4×10^5	0.025	7.80	25	32	100.0	2.4	27	147	8.10	0.830	4.06×10^5	1.23	574
								5.7	28	148	8.50	.834	4.61	1.27	589
								8.9	29	178	8.96	.677	5.26	1.35	490
								12.1	31	184	9.50	.654	6.02	1.49	489
								15.3	32	214	10.3	.547	6.92	1.75	424
								18.5	32	233	11.0	.501	7.97	2.24	403
266	13.7×10^5	13.6×10^5	0.034	10.2	24	26	9.8	2.4	24	31	10.2	1.540	4.71×10^5	1.21	1049
								5.7	25	33	10.2	1.252	4.76	↓	854
								8.9	↓	31	10.3	1.620	4.80		1105
								12.1		31	10.3	1.830	4.85		1248
								15.3		31	10.4	1.880	4.90	1.22	1285
								18.5	26	30	10.4	2.160	4.95	1.22	1481
267	13.5×10^5	13.4×10^5	0.034	10.2	24	28	44.0	2.4	25	54	10.3	1.520	4.83×10^5	1.21	1038
								5.7	26	57	10.4	1.390	5.04	1.22	956
								8.9	26	62	10.6	1.240	5.26	1.22	858
								12.1	27	66	10.8	1.136	5.49	1.23	791
								15.3	27	68	10.9	1.074	5.73	1.25	753
								18.5	28	80	11.2	.845	5.98	1.26	597
268	13.5×10^5	13.4×10^5	0.033	10.1	24	32	100.0	2.4	26	136	10.3	0.898	4.95×10^5	1.22	616
								5.7	27	166	10.6	.712	5.46	1.24	497
								8.9	28	158	11.1	.762	6.02	1.27	540
								12.1	29	165	15.5	.736	6.66	1.34	530
								15.3	31	226	12.0	.510	7.38	1.43	375
								18.5	31	223	12.6	.515	8.20	1.57	390

TABLE II. - Continued. NEAR CRITICAL HYDROGEN DATA

[Inconel X tube: inside diameter, 0.311 in. (0.790 cm); outside diameter, 0.331 in. (0.840 cm).]

(a-2) Concluded. Straight inlet; SI units

Run	Inlet pressure, p_{in}, N/m^2	Outlet pressure, p_{out}, N/m^2	Flow rate, $\dot{\omega}$, kg/sec	Inlet velocity, V_{in}, m/sec	Inlet bulk temperature, $T_{b,in}$, K	Outlet bulk temperature, $T_{b,out}$, K	Heat flux, q, W/cm^2	x/d	Bulk temperature, T_b, K	Inside surface wall temperature, $T_{w,i}$, K	Bulk velocity, V_b, m/sec	Heat transfer coefficient, h, $W/(cm^2)(K)$	Bulk Reynolds number, Re_b	Bulk Prandtl number, Pr_b	Bulk Nusselt number, Nu_b
270	20.4×10^5	20.4×10^5	0.016	4.94	26	28	9.8	2.4	26	35	4.97	1.070	2.37×10^5	1.21	727
								5.7	27	37	5.00	.871	2.42	1.21	596
								8.9	↓	33	5.03	1.436	2.46	1.21	983
								12.1		36	5.06	1.102	2.51	1.22	757
								15.3		36	5.13	1.140	2.55	1.22	784
								18.5	28	38	5.15	.919	2.60	1.22	634
271	20.3×10^5	20.3×10^5	0.014	4.27	27	33	44.0	2.4	28	86	4.42	0.765	2.24×10^5	1.22	529
								5.7	29	95	4.57	.668	2.47	1.25	468
								8.9	31	111	4.75	.554	2.73	1.29	395
								12.1	32	136	4.97	.427	3.02	1.34	310
								15.3	33	136	5.21	.427	3.35	1.42	319
								18.5	33	129	5.50	.426	3.71	1.53	355
272	20.8×10^5	20.8×10^5	0.015	4.45	26	37	98.0	2.4	28	139	4.73	0.895	2.46×10^5	1.23	622
								5.7	31	136	5.15	.945	3.04	1.31	683
								8.9	33	162	5.70	.769	3.77	1.48	583
								12.1	34	163	6.40	.769	4.67	1.76	620
								15.3	36	176	7.38	.706	5.67	2.32	615
								18.5	37	194	8.60	.630	6.67	2.27	592
273	20.1×10^5	20.1×10^5	0.016	4.48	26	40	165.0	2.4	29	173	5.37	1.150	2.95×10^5	1.26	812
								5.7	33	175	6.22	1.168	4.10	1.48	882
								8.9	35	190	7.50	1.070	5.66	2.05	894
								12.1	36	219	9.52	.900	7.37	2.40	853
								15.3	37	227	12.20	.868	8.69	1.82	898
275	20.3×10^5	20.2×10^5	0.032	9.75	26	27	9.8	2.4	26	32	9.82	1.592	4.56×10^5	1.21	1078
								5.7	↓	33	9.85	1.371	4.60	↓	931
								8.9		32	9.90	1.529	4.65		1037
								12.1		31	9.92	2.148	4.69		1464
								15.3		31	9.95	1.970	4.73		1342
								18.5	27	35	10.00	1.111	4.78		758

276	20.3×10^5	20.2×10^5	0.033	9.90	26	29	46.0	2.4	26	45	10.00	2.390	4.74×10^5	1.21	1625
								5.7	27	49	10.20	1.990	4.95	1.21	1364
								8.9	27	55	10.30	1.640	5.17	1.22	1129
								12.1	28	60	10.50	1.420	5.39	1.22	981
								15.3	29	64	10.70	1.285	5.63	1.23	895
								18.5	29	73	10.90	1.040	5.87	1.25	730
277	20.2×10^5	20.1×10^5	0.033	10.20	26	33	100.0	2.4	27	116	10.40	1.111	5.05×10^5	1.21	761
								5.7	28	125	10.80	1.028	5.54	1.22	712
								8.9	29	132	11.20	.970	6.07	1.25	681
								12.1	31	142	11.60	.892	6.66	1.29	638
								15.3	32	148	12.10	.856	7.32	1.34	625
								18.5	32	168	12.60	.733	8.05	1.41	546
278	20.0×10^5	19.9×10^5	0.032	10.20	26	35	164.0	2.4	28	166	10.60	1.190	5.41×10^5	1.22	825
								5.7	30	177	11.30	1.116	6.31	1.27	792
								8.9	32	202	12.00	.965	7.39	1.36	708
								12.1	33	213	13.00	.913	8.67	1.51	694
								15.3	34	227	14.20	.850	10.16	1.73	678
								18.5	35	273	15.7	.690	11.81	2.08	579
280	20.6×10^5	20.4×10^5	0.047	14.10	24	26	9.8	2.4	24	29	14.10	2.200	6.21×10^5	1.21	1478
								5.7	24	31	14.10	1.480	6.25	1.21	997
								8.9	25	30	14.20	1.830	6.29	1.22	1230
								12.1	↓	28	14.20	2.770	6.34	↓	1860
								15.3		29	14.30	2.460	6.38		1650
								18.5		32	14.30	1.460	6.42		982
281	20.1×10^5	20.1×10^5	0.046	14.00	25	28	44.0	2.4	26	43	14.20	2.540	6.50×10^5	1.22	1716
								5.7	26	43	14.40	2.610	6.70	1.21	1773
								8.9	27	43	14.50	2.680	6.90	1.21	1831
								12.1	27	44	14.60	2.580	7.11	1.21	1769
								15.3	27	43	14.70	2.842	7.32	1.22	1955
								18.5	28	47	14.90	2.330	7.54	1.22	1607
282	19.8×10^5	19.7×10^5	0.047	14.20	25	31	98.0	2.4	26	91	14.40	1.490	6.73×10^5	1.21	1013
								5.7	27	107	14.70	1.220	7.19	1.21	836
								8.9	28	128	15.10	.875	7.66	1.22	674
								12.1	29	117	15.50	1.108	8.17	1.24	774
								15.3	29	110	15.80	1.219	8.71	1.26	862
								18.5	31	126	16.30	1.020	9.30	1.29	727
283	20.2×10^5	20.0×10^5	0.043	13.10	26	33	162.0	2.4	27	171	13.50	1.120	6.61×10^5	1.21	769
								5.7	29	189	14.10	1.008	7.43	1.23	702
								8.9	30	207	14.80	.960	8.34	1.28	645
								12.1	32	229	15.10	.821	9.40	1.34	598
								15.3	33	268	16.40	.689	10.60	1.44	517
								18.5	33	291	17.50	.630	11.96	1.57	487

TABLE II. - Continued. NEAR CRITICAL HYDROGEN DATA

[Inconel X tube: inside diameter, 0.311 in. (0.790 cm); outside diameter, 0.331 in. (0.840 cm).]

(b-1) Plenum inlet; U. S. customary units

Run	Inlet pressure, p_{in}, lb/in.^{2}	Outlet pressure, p_{out}, lb/in.^{2}	Flow rate, $\dot{\omega}$, lb/sec	Inlet velocity, V_{in}, ft/sec	Inlet bulk temperature, $T_{b,in}$, ^oR	Outlet bulk temperature, $T_{b,out}$, ^oR	Heat flux, q, $\frac{Btu}{(sec)(in.^2)}$	x/d	Bulk temperature, T_b, ^oR	Inside surface wall temperature, $T_{w,i}$, ^oR	Bulk velocity, V_b, ft/sec	Heat transfer coefficient, h, $\frac{Btu}{(sec)(in.^2)(^oR)}$	Bulk Reynolds number, Re_b	Bulk Prandtl number, Pr_b	Bulk Nusselt number, Nu_b
146	189	189	0.022	11.1	51	56	0.06	2.4	52	82	11.2	2.10×10^{-3}	1.90×10^5	1.30	442
								5.7	52	89	11.3	1.74	1.97	1.32	368
								8.9	53	95	11.5	1.52	2.04	1.35	324
								12.1	54	109	11.7	1.15	2.11	1.38	248
								15.3	54	95	11.8	1.57	2.19	1.41	339
								18.5	55	102	12.0	1.35	2.27	1.45	295
147	212	212	0.023	11.3	50	61	0.28	2.4	52	151	11.8	2.79×10^{-3}	2.02×10^5	1.30	586
								5.7	55	142	12.5	3.16	2.33	1.41	684
								8.7	57	153	13.4	2.87	2.71	1.60	643
								12.1	59	160	14.5	2.71	3.15	1.97	635
								15.3	60	153	15.8	2.95	3.66	2.76	726
								18.5	60	177	17.6	2.36	4.23	5.75	616
157	200	199	0.030	14.4	48	51	0.06	2.4	49	70	14.6	2.90×10^{-3}	2.27×10^5	1.23	596
								5.7	49	66	14.7	3.70	2.33	1.24	760
								8.9	50	71	14.8	2.93	2.38	1.25	605
								12.1	50	77	15.0	2.34	2.44	1.26	484
								15.3	51	69	15.1	3.43	2.50	1.27	714
								18.5	51	77	15.3	2.43	2.56	1.28	509
158	190	190	0.032	14.9	47	58	0.28	2.4	49	119	15.3	3.95×10^{-3}	2.43×10^5	1.24	813
								5.7	51	116	15.9	4.28	2.69	1.29	896
								8.9	53	130	16.6	3.61	2.99	1.36	772
								12.1	55	139	17.4	3.30	3.33	1.48	722
								15.3	57	134	18.4	3.57	3.73	1.66	804
								18.5	58	156	19.5	2.81	4.18	1.97	654
153	199	198	0.056	25.9	45	48	0.06	2.4	45	62	25.9	3.68×10^{-3}	3.74×10^5	1.22	741
								5.7	46	58	26.0	4.98	3.78		1003
								8.9	46	62	26.2	3.84	3.83		776
								12.1	46	66	26.3	3.13	3.88		633
								15.3	47	57	26.4	5.95	3.93		1207
								18.5	47	62	26.5	4.10	3.98		833

154	197	196	0.057	26.2	45	53	0.28	2.4	46	89	26.6	6.41×10^{-3}	3.91×10^{5}	1.22	1297
								5.7	48	92	27.1	6.20	4.14	1.23	1263
								8.9	49	113	27.6	4.30	4.38	1.24	884
								12.1	50	129	28.2	3.49	4.63	1.26	725
								15.3	52	119	28.9	4.08	4.90	1.29	855
								18.5	53	130	29.6	3.56	5.19	1.33	754
155	195	194	0.056	26.0	45	59	0.62	2.4	48	196	26.7	4.17×10^{-3}	4.09×10^{5}	1.23	850
								5.7	51	197	28.1	4.23	4.64	1.27	880
								8.9	53	210	29.6	3.95	5.30	1.36	842
								12.1	55	223	31.4	3.69	6.07	1.50	812
								15.3	57	222	33.6	3.75	6.98	1.76	855
								18.5	58	255	36.3	3.15	8.05	2.27	748
149	198	196	0.071	33.2	47	48	0.06	2.4	47	62	33.4	4.15×10^{-3}	5.05×10^{5}	1.22	844
								5.7	48	55	33.5	8.15	5.10	1.22	1660
								8.9	↓	60	33.7	5.01	5.15	1.23	1021
								12.1		65	33.8	3.61	5.21	↓	737
								15.3		56	33.9	7.91	5.26		1619
								18.5	49	61	34.0	4.91	5.31		1006
150	198	196	0.071	33.4	47	53	0.27	2.4	48	84	33.9	7.58×10^{-3}	5.21×10^{5}	1.23	1548
								5.7	49	87	34.4	7.21	5.44	1.24	1481
								8.9	50	99	35.0	5.60	5.69	1.26	1159
								12.1	51	117	35.6	4.16	5.96	1.28	867
								15.3	52	114	36.3	4.42	6.23	1.30	930
								18.5	53	128	37.0	3.65	6.53	1.34	775
151	198	196	0.071	33.2	47	58	0.62	2.4	49	181	34.1	4.67×10^{-3}	5.39×10^{5}	1.24	960
								5.7	51	187	35.5	4.55	5.97	1.28	951
								8.9	53	198	37.0	4.27	6.63	1.35	910
								12.1	55	219	38.8	3.76	7.38	1.46	822
								15.3	57	215	40.9	3.90	8.24	1.63	874
								18.5	58	247	43.2	3.26	9.23	1.90	755
152	195	192	0.070	33.2	48	60	1.11	2.4	51	336	35.2	3.90×10^{-3}	5.93×10^{5}	1.29	816
								5.7	55	358	38.2	3.66	7.19	1.44	797
								8.9	57	413	42.0	3.12	8.80	1.80	715
								12.1	59	447	47.2	2.86	10.82	2.81	700
								15.3	60	498	54.4	2.54	13.52	12.70	674
								18.5	60	564	64.2	2.20	15.82	19.50	639
159	298	297	0.033	15.6	48	52	0.06	2.4	48	68	15.6	3.23×10^{-3}	2.33×10^{5}	1.21	651
								5.7	49	64	15.8	4.22	2.33	1.22	853
								8.9	50	73	15.9	2.70	2.43	↓	548
								12.1	50	77	16.0	2.36	2.48		479
								15.3	51	68	16.1	3.66	2.53		746
								18.5	51	74	16.3	2.78	2.58	1.23	569

TABLE II. - Continued. NEAR CRITICAL HYDROGEN DATA

[Inconel X tube: inside diameter, 0.311 in. (0.790 cm); outside diameter, 0.331 in. (0.840 cm).]

(b-1) Concluded. Plenum inlet; U. S. customary units

Run	Inlet pressure, p_{in}, lb/in.^{2}	Outlet pressure, p_{out}, lb/in.^{2}	Flow rate, $\dot{\omega}$, lb/sec	Inlet velocity, V_{in}, ft/sec	Inlet bulk temperature, $T_{b,in}$, ^oR	Outlet bulk temperature, $T_{b,out}$, ^oR	Heat flux, q, $\frac{Btu}{(sec)(in.^2)}$	x/d	Bulk temperature, T_b, ^oR	Inside surface wall temperature, $T_{w,i}$, ^oR	Bulk velocity, V_b, ft/sec	Heat transfer coefficient, h, $\frac{Btu}{(sec)(in.^2)(^oR)}$	Bulk Reynolds number, Re_b	Bulk Prandtl number, Pr_b	Bulk Nusselt number, Nu_b
160	295	295	0.031	14.6	48	61	0.28	2.4	50	104	14.9	5.23×10^{-3}	2.31×10^5	1.22	1064
								5.7	53	111	15.5	4.83	2.55	1.25	998
								8.9	55	115	16.2	4.69	2.83	1.29	987
								12.1	57	129	16.9	3.91	3.13	1.35	840
								15.3	58	126	17.7	4.19	3.47	1.43	921
								18.5	60	150	18.7	3.14	3.85	1.53	709
162	303	302	0.075	32.6	42	44	0.06	2.4	42	55	32.6	4.49×10^{-3}	4.17×10^5	1.21	880
								5.7	43	50	32.7	7.67	4.21	1.20	1503
								8.9	↓	57	32.8	4.02	4.24	1.20	789
								12.1	↓	62	32.8	3.03	4.28	1.21	594
								15.3	↓	53	32.9	5.92	4.33	1.21	1164
								18.5	44	58	33.0	3.98	4.37	1.21	784
163	303	301	0.073	32.0	42	50	0.28	2.4	43	80	32.1	7.45×10^{-3}	4.19×10^5	1.21	1464
								5.7	44	83	32.6	7.14	4.39	1.22	1410
								8.9	46	84	33.0	7.19	4.59	1.22	1429
								12.1	47	99	33.5	5.30	4.80	1.21	1058
								15.3	48	94	34.0	6.01	5.01	1.21	1208
								18.5	49	105	34.5	4.95	5.22	1.22	1001
164	302	300	0.075	32.8	42	57	0.63	2.4	44	155	33.5	5.70×10^{-3}	4.50×10^5	1.21	1125
								5.7	47	158	34.5	5.69	4.97	1.21	1138
								8.9	50	169	35.7	5.29	5.46	1.22	1072
								12.1	52	185	36.9	4.75	5.98	1.23	976
								15.3	54	179	38.3	5.06	6.57	1.27	1057
								18.5	56	200	39.9	4.39	7.22	1.32	934

165	21.0×10^5	20.8×10^5	0.033	9.72	24	36	183.0	2.4	26	132	10.19	1.741	4.80×10^5	1.21	1182
								5.7	29	137	10.80	1.692	5.69	1.23	1179
								8.9	31	144	11.60	1.630	6.75	1.30	1168
								12.1	33	154	12.55	1.520	8.05	1.41	1131
								15.3	34	152	13.75	1.555	9.59	1.60	1215
								18.5	35	172	15.25	1.346	11.34	1.87	1111
166	21.8×10^5	21.5×10^5	0.045	13.42	24	26	9.8	2.4	24	28	13.42	2.700	5.88×10^5	1.21	1806
								5.7	24	28	13.42	3.290	5.92	1.22	2203
								8.9	25	31	13.45	1.774	5.97	↓	1190
								12.1	↓	33	13.49	1.300	6.02		874
								15.3		29	13.51	2.660	6.06		1784
								18.5		31	13.55	1.720	6.11		1156
167	21.4×10^5	21.2×10^5	0.047	14.11	25	28	46.0	2.4	26	44	14.30	2.380	6.52×10^5	1.22	1604
								5.7	26	39	14.38	3.490	6.73	1.21	2360
								8.9	26	45	14.62	2.440	6.93	↓	1654
								12.1	27	48	14.80	2.170	7.14		1478
								15.3	27	39	14.92	3.730	7.36		2558
								18.5	28	44	15.10	2.720	7.58	1.22	1869
168	21.4×10^5	21.2×10^5	0.046	13.90	26	31	104.0	2.4	27	76	14.26	2.100	6.78×10^5	1.21	1427
								5.7	28	91	14.60	1.655	7.27	1.22	1136
								8.9	28	103	15.00	1.392	7.78	1.23	967
								12.1	29	108	15.50	1.320	8.34	1.24	928
								15.3	31	103	15.80	1.440	8.94	1.27	1024
								18.5	31	127	16.30	1.092	9.59	1.30	787
169	21.2×10^5	20.8×10^5	0.047	14.29	25	34	180.0	2.4	26	142	14.60	1.560	6.99×10^5	1.21	1060
								5.7	28	159	15.23	1.380	7.85	1.22	955
								8.9	30	169	15.82	1.294	8.82	1.26	915
								12.1	31	164	16.80	1.354	9.93	1.31	977
								15.3	32	155	17.70	1.470	11.20	1.39	1090
								18.5	33	182	18.90	1.226	12.64	1.50	926

TABLE II. - Continued. NEAR CRITICAL HYDROGEN DATA

[Inconel X tube: inside diameter, 0.311 in. (0.790 cm); outside diameter, 0.331 in. (0.840 cm).]

(b-2) Plenum inlet; SI units

Run	Inlet pressure, p_{in}, N/m^2	Outlet pressure, p_{out}, N/m^2	Flow rate, $\dot{\omega}$, kg/sec	Inlet velocity, V_{in}, m/sec	Inlet bulk temperature, $T_{b,in}$, K	Outlet bulk temperature, $T_{b,out}$, K	Heat flux, q, W/cm^2	x/d	Bulk temperature, T_b, K	Inside surface wall temperature, $T_{w,i}$, K	Bulk velocity, V_b, K	Heat transfer coefficient, h, $W/(cm^2)(K)$	Bulk Reynolds number, Re_b	Bulk Prandtl number, Pr_b	Bulk Nusselt number, Nu_b
146	13.0×10^5	13.0×10^5	0.010	3.38	28	31	9.8	2.4	29	46	3.41	0.618	1.90×10^5	1.30	442
								5.7	29	49	3.44	.513	1.97	1.32	368
								8.9	29	53	3.50	.448	2.04	1.35	324
								12.1	30	61	3.56	.338	2.11	1.38	248
								15.3	30	53	3.60	.462	2.19	1.41	339
								18.5	31	57	3.66	.398	2.27	1.45	295
147	14.6×10^5	14.6×10^5	0.010	3.44	28	34	46.0	2.4	29	84	3.60	0.822	2.02×10^5	1.30	586
								5.7	31	79	3.81	.930	2.33	1.41	684
								8.9	32	85	4.09	.845	2.71	1.60	643
								12.1	33	89	4.42	.798	3.15	1.97	635
								15.3	33	85	4.82	.870	3.66	2.76	726
								18.5	33	98	5.36	.695	4.23	5.75	616
157	13.8×10^5	13.7×10^5	0.014	4.39	27	28	9.8	2.4	27	39	4.45	0.854	2.27×10^5	1.23	596
								5.7	27	37	4.48	1.090	2.33	1.24	760
								8.9	28	39	4.51	.863	2.38	1.25	605
								12.1	↓	43	4.57	.690	2.44	1.26	484
								15.3		38	4.60	1.010	2.50	1.27	714
								18.5		43	4.66	.716	2.56	1.28	509
158	13.1×10^5	13.1×10^5	0.015	4.54	26	32	46.0	2.4	27	66	4.66	1.162	2.43×10^5	1.24	813
								5.7	28	64	4.85	1.260	2.69	1.29	896
								8.9	29	72	5.06	1.062	2.99	1.36	772
								12.1	31	77	5.30	.972	3.33	1.48	722
								15.3	32	74	5.61	1.050	3.73	1.66	804
								18.5	32	87	5.95	.827	4.18	1.97	654
153	13.7×10^5	13.6×10^5	0.025	7.90	25	27	9.8	2.4	25	34	7.90	1.082	3.74×10^5	1.22	741
								5.7	26	32	7.93	1.468	3.78	↓	1003
								8.9	↓	34	7.99	1.130	3.83		776
								12.1		37	8.02	.922	3.88		633
								15.3		32	8.05	1.750	3.93		1207
								18.5		34	8.08	1.208	3.98		833

154	13.6×10^5	13.5×10^6	0.026	7.99	25	29	46.0	2.4	26	49	8.16	1.890	3.91×10^5	1.22	1297
								5.7	27	51	8.26	1.828	4.14	1.23	1263
								8.9	27	63	8.40	1.265	4.38	1.24	884
								12.1	28	72	8.50	1.030	4.63	1.26	725
								15.3	29	66	8.80	1.200	4.90	1.29	855
								18.5	29	72	9.02	1.050	5.19	1.33	754
155	13.4×10^5	13.4×10^5	0.025	7.92	25	33	101.0	2.4	27	109	8.15	1.230	4.09×10^5	1.23	850
								5.7	28	109	8.56	1.245	4.64	1.27	880
								8.9	29	117	9.02	1.162	5.30	1.36	842
								12.1	31	124	9.57	1.088	6.07	1.50	812
								15.3	32	123	10.24	1.108	6.98	1.76	855
								18.5	32	142	11.08	.928	8.05	2.27	748
149	13.7×10^5	13.5×10^5	0.032	10.11	26	27	9.8	2.4	26	34	10.19	1.220	5.05×10^5	1.22	844
								5.7	27	31	10.21	2.400	5.10	1.22	1660
								8.9	↓	33	10.28	1.475	5.15	1.23	1021
								12.1		36	10.30	1.062	5.21	↓	737
								15.3		31	10.32	2.330	5.26		1619
								18.5		34	10.36	1.448	5.31		1006
150	13.7×10^5	13.5×10^5	0.032	10.19	26	29	44.0	2.4	27	47	10.32	2.230	5.21×10^5	1.23	1548
								5.7	27	48	10.49	2.122	5.44	1.24	1481
								8.9	28	55	10.51	1.650	5.69	1.26	1159
								12.1	28	65	10.53	1.226	5.96	1.28	867
								15.3	29	63	11.08	1.300	6.23	1.30	930
								18.5	29	71	11.29	1.074	6.53	1.34	775
151	13.7×10^5	13.5×10^5	0.032	10.11	26	32	101.0	2.4	26	101	10.40	1.372	5.39×10^5	1.24	960
								5.7	28	104	10.82	1.340	5.97	1.28	951
								8.9	29	110	11.60	1.254	6.63	1.35	910
								12.1	31	122	11.82	1.110	7.38	1.46	822
								15.3	32	102	12.46	1.112	8.24	1.63	874
								18.5	32	137	13.19	.960	9.23	1.90	755
152	13.5×10^5	13.2×10^5	0.032	10.10	27	33	181.0	2.4	28	187	10.72	1.150	5.93×10^5	1.29	816
								5.7	31	199	11.63	1.079	7.19	1.44	797
								8.9	32	229	12.80	.920	8.80	1.80	715
								12.1	33	248	14.40	.814	10.82	2.81	700
								15.3	33	277	16.58	.749	13.25	12.70	674
								18.5	33	313	19.60	.648	15.82	19.50	639
159	20.6×10^5	20.5×10^5	0.015	4.75	27	29	9.8	2.4	27	38	4.75	0.952	2.33×10^5	1.21	651
								5.7	27	35	4.82	1.242	2.38	1.22	853
								8.9	28	41	4.85	.795	2.43	↓	548
								12.1	↓	43	4.88	.695	2.48		479
								15.3		38	4.90	1.079	2.53		746
								18.5		41	4.97	.820	2.58	1.23	569

TABLE II. - Concluded. NEAR CRITICAL HYDROGEN DATA

[Inconel X tube: inside diameter, 0.311 in. (0.790 cm); outside diameter, 0.331 in. (0.840 cm).]

(b-2) Concluded. Plenum inlet; SI units

Run	Inlet pressure, p_{in}, N/m^2	Outlet pressure, p_{out}, N/m^2	Flow rate, $\dot{\omega}$, kg/sec	Inlet velocity, V_{in}, m/sec	Inlet bulk temperature, $T_{b,in}$, K	Outlet bulk temperature, $T_{b,out}$, K	Heat flux, q, W/cm^2	x/d	Bulk temperature, T_b, m/sec	Inside surface wall temperature, $T_{w,i}$, K	Bulk velocity, V_b, m/sec	Heat transfer coefficient, h, $W/(cm^2)(K)$	Bulk Reynolds number, Re_b	Bulk Prandtl number, Pr_b	Bulk Nusselt number, Nu_b
160	20.4×10^5	20.4×10^5	0.014	4.45	27	34	46.0	2.4	28	57	4.54	1.540	2.31×10^5	1.22	1064
								5.7	29	62	4.72	1.422	2.55	1.25	998
								8.9	31	64	4.94	1.380	2.83	1.29	987
								12.1	32	72	5.15	1.150	3.13	1.35	840
								15.3	32	70	5.40	1.230	3.47	1.43	921
								18.5	33	83	5.70	.925	3.85	1.53	709
162	20.9×10^5	20.8×10^5	0.034	9.94	23	24	9.8	2.4	23	31	9.94	1.320	4.17×10^5	1.21	880
								5.7	24	28	9.96	2.260	4.21	1.20	1503
								8.9	↓	32	10.00	1.182	4.24	1.20	789
								12.1		34	10.00	.892	4.28	1.21	594
								15.3		29	10.02	1.740	4.33	1.21	1164
								18.5		32	10.07	1.171	4.37	1.21	784
163	20.9×10^5	20.8×10^5	0.033	9.75	23	28	46.0	2.4	24	44	9.78	2.198	4.19×10^5	1.21	1464
								5.7	24	46	9.94	2.100	4.39	1.22	1410
								8.9	26	47	10.07	2.163	4.59	1.22	1429
								12.1	26	55	10.20	1.560	4.80	1.21	1058
								15.3	27	52	10.38	1.770	5.01	1.21	1208
								18.5	27	58	10.50	1.460	5.22	1.22	1001
164	20.8×10^5	20.7×10^5	0.034	10.00	23	32	103.0	2.4	24	86	10.20	1.680	4.50×10^5	1.21	1125
								5.7	26	88	10.50	1.675	4.97	1.21	1138
								8.9	28	94	10.88	1.560	5.46	1.22	1072
								12.1	29	103	11.22	1.400	5.98	1.23	976
								15.3	30	100	11.70	1.490	6.57	1.27	1057
								18.5	31	111	12.18	1.291	7.22	1.32	934

165	304	302	0.073	31.9	43	64	1.12	2.4	47	237	33.4	5.92×10^{-3}	4.80×10^{5}	1.21	1182
								5.7	52	247	35.5	5.75	5.69	1.23	1179
								8.9	56	259	38.1	5.53	6.75	1.30	1168
								12.1	59	277	41.2	5.15	8.05	1.41	1131
								15.3	61	274	45.1	5.28	9.59	1.60	1215
								18.5	63	309	50.0	4.57	11.34	1.87	1111
166	315	312	0.099	44.1	44	46	0.06	2.4	44	51	44.0	9.16×10^{-3}	5.88×10^{5}	1.21	1806
								5.7	44	50	44.1	11.16	5.92	1.22	2203
								8.9	45	55	44.2	6.03	5.97	↓	1190
								12.1	↓	59	44.3	4.42	6.02	↓	874
								15.3	↓	52	44.4	9.02	6.06	↓	1784
								18.5	↓	56	44.5	5.84	6.11	↓	1156
167	311	307	0.104	46.4	45	50	0.28	2.4	46	80	47.0	8.08×10^{-3}	6.52×10^{5}	1.22	1604
								5.7	47	70	47.5	11.84	6.73	1.21	2360
								8.9	47	81	48.0	8.27	6.93	↓	1654
								12.1	48	86	48.5	7.36	7.14	↓	1478
								15.3	49	71	49.0	12.68	7.36	↓	2558
								18.5	50	80	49.5	9.22	7.58	1.22	1869
168	311	307	0.101	45.7	46	56	0.64	2.4	48	137	46.8	7.13×10^{-3}	6.78×10^{5}	1.21	1427
								5.7	50	163	47.9	5.62	7.27	1.22	1136
								8.9	51	186	49.2	4.74	7.78	1.23	967
								12.1	53	195	50.5	4.49	8.34	1.24	928
								15.3	55	185	51.9	4.89	8.94	1.27	1024
								18.5	56	228	53.5	3.71	9.59	1.30	787
169	307	302	0.104	46.8	45	61	1.10	2.4	47	256	48	5.29×10^{-3}	6.99×10^{5}	1.21	1060
								5.7	51	286	50	4.69	7.85	1.22	955
								8.9	54	304	52	4.40	8.82	1.26	915
								12.1	56	296	55	4.60	9.93	1.31	977
								15.3	58	279	58	5.00	11.20	1.39	1090
								18.5	60	328	62	4.16	12.64	1.50	926

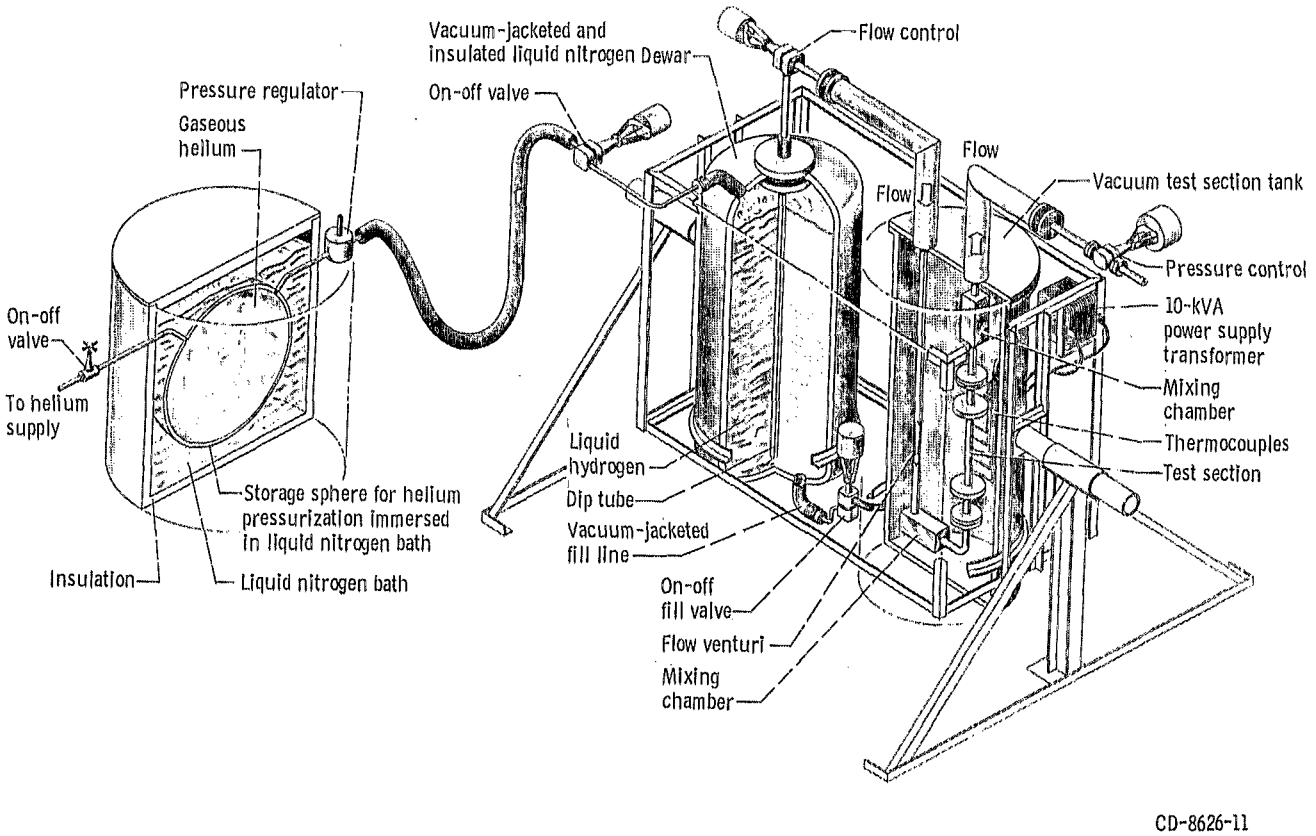

Figure 1. - Liquid hydrogen heat transfer apparatus.

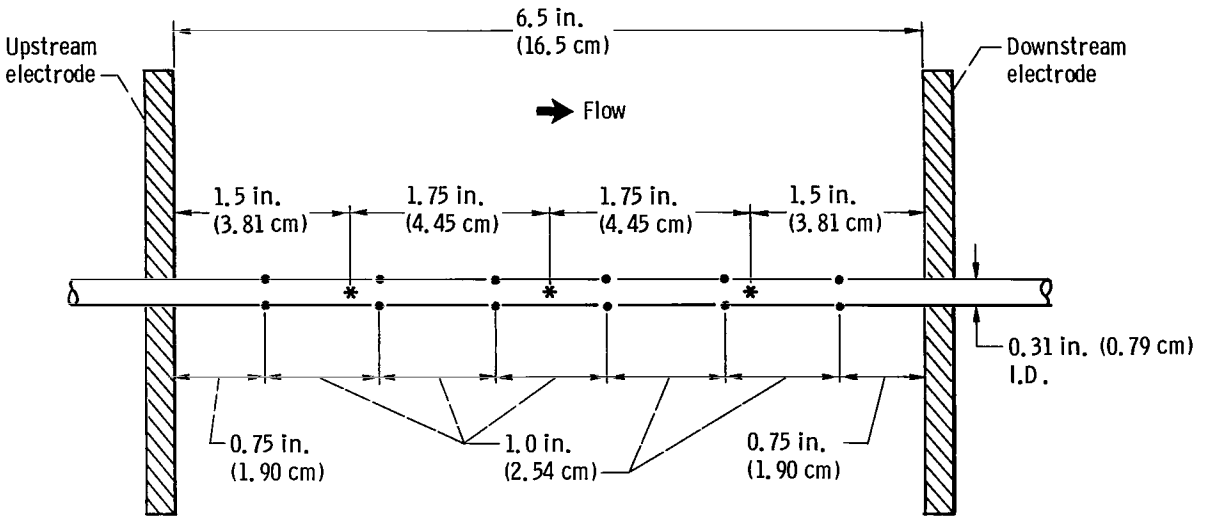

• Surface thermocouple
* Local voltage tap

(a) Heated length.

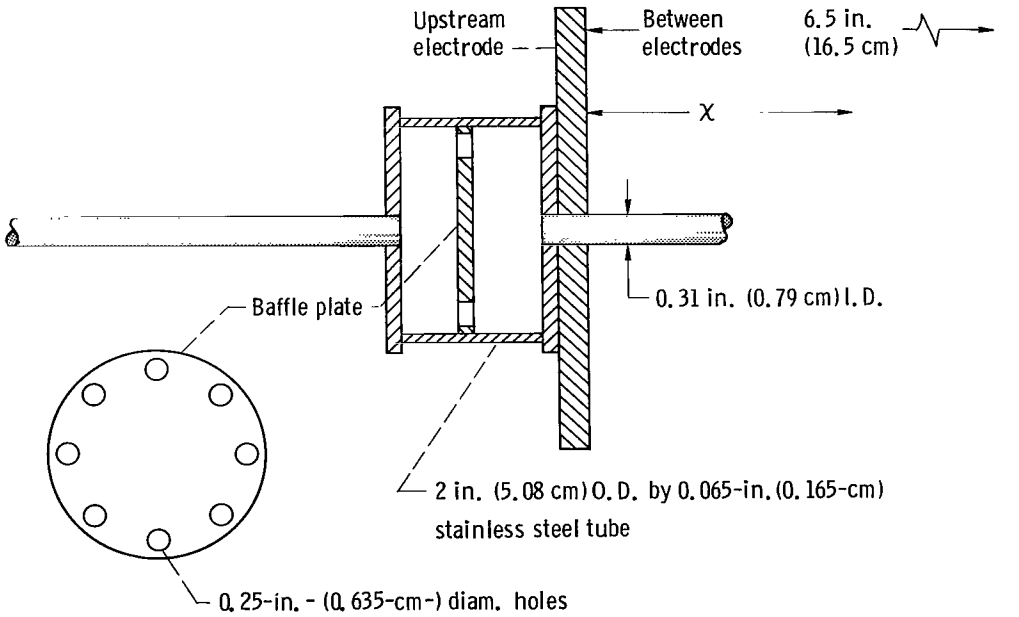

(b) Plenum inlet.

Figure 2. - Test section.

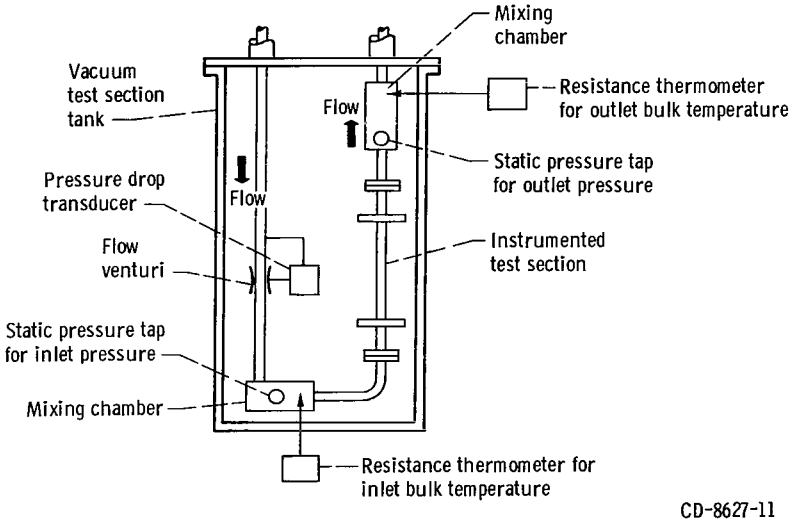

Figure 3. - Flow system instrumentation.

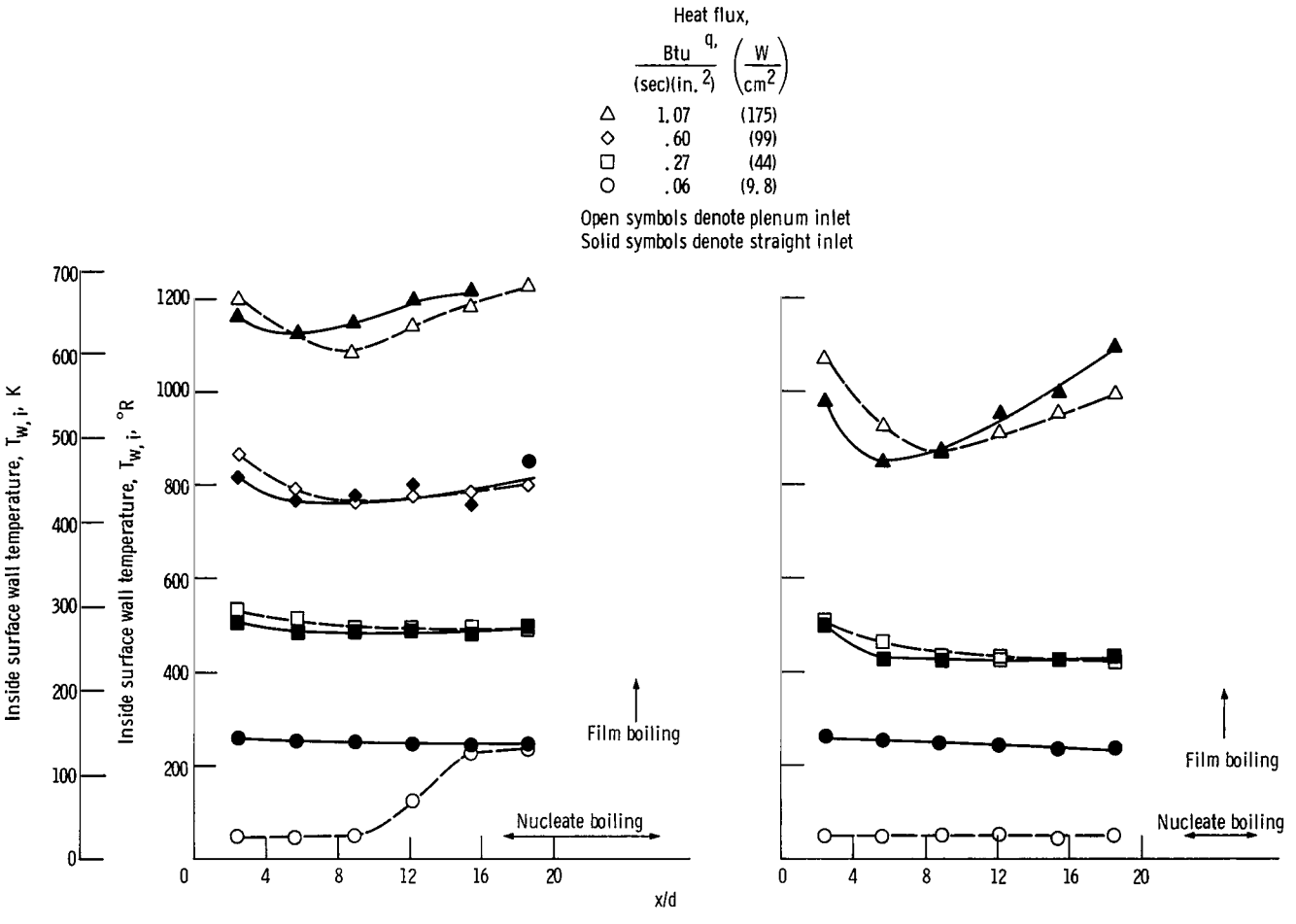

(a) Inlet velocity, 10.5 feet per second (3.2 m/sec).

(b) Inlet velocity, 15 feet per second (4.6 m/sec).

Figure 4. - Liquid hydrogen boiling data for various inlet velocities. Absolute pressure, 50 psi (3.4×10^5 N/m^2); tube diameter, 0.31 inch (0.79 cm).

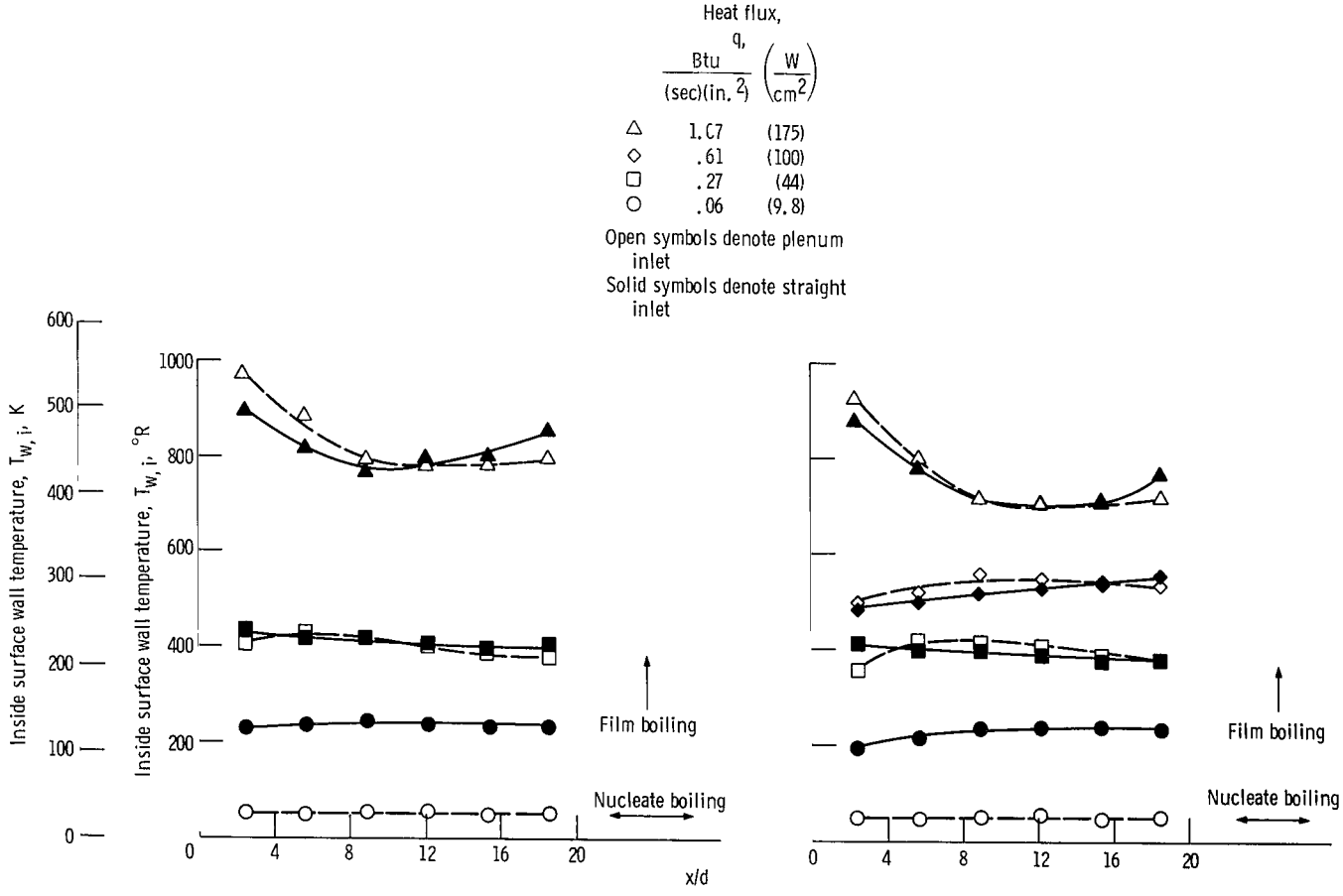

(c) Inlet velocity, 26 feet per second (7.9 m/sec).

(d) Inlet velocity, 33 feet per second (10.1 m/sec).

Figure 4. - Continued.

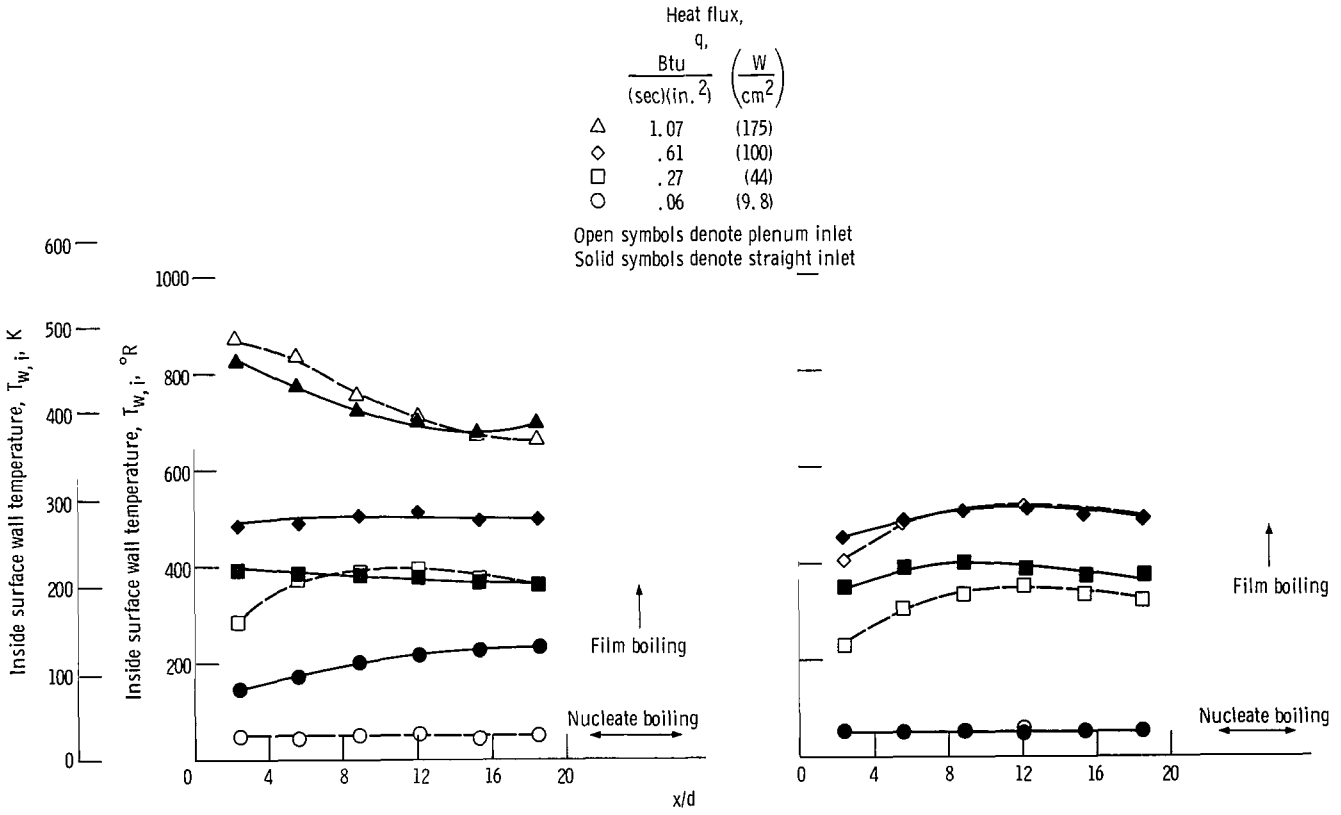

(e) Inlet velocity, 47 feet per second (14.3 m/sec).

(f) Inlet velocity, 67 feet per second (20.4 m/sec).

Figure 4. - Concluded.

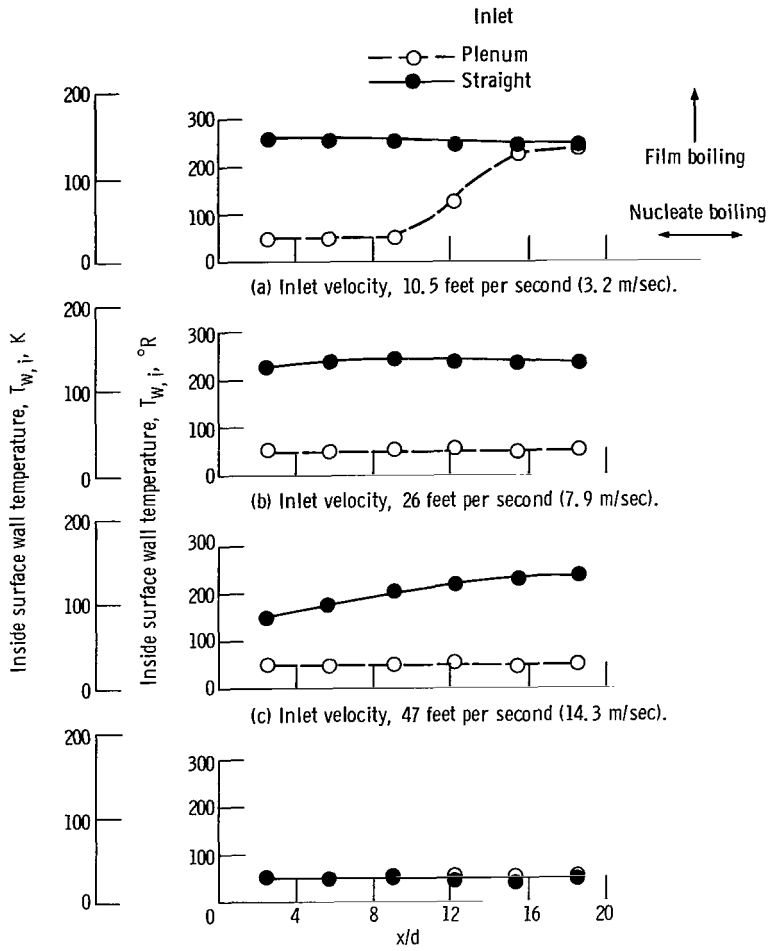

(a) Inlet velocity, 10.5 feet per second (3.2 m/sec).

(b) Inlet velocity, 26 feet per second (7.9 m/sec).

(c) Inlet velocity, 47 feet per second (14.3 m/sec).

(d) Inlet velocity, 67 feet per second (20.4 m/sec).

Figure 5. - Inlet effect on transition from nucleate to film boiling for liquid hydrogen. Absolute pressure, 50 psi (3.4×10^5 N/m^2); tube diameter, 0.31 inch (0.79 cm); heat flux, 0.06 Btu/(sec)(in.^{2}) (9.8 W/cm^2).

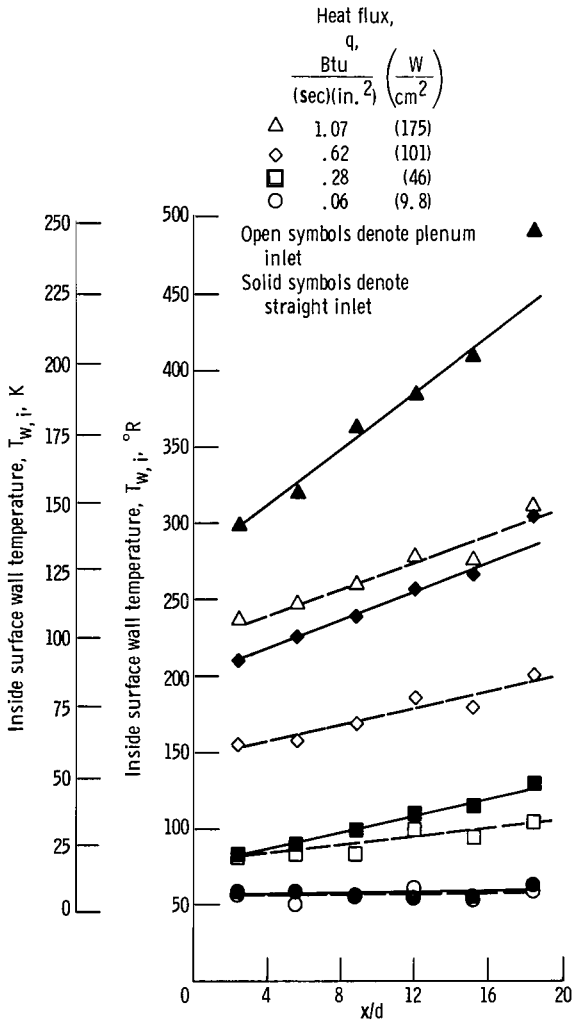

Figure 6. - Near critical hydrogen data. Absolute pressure, 300 psi (20.7x10^5 N/m^2); inlet velocity, 32 feet per second (9.8 m/sec); tube diameter, 0.31 inch (0.79 cm).

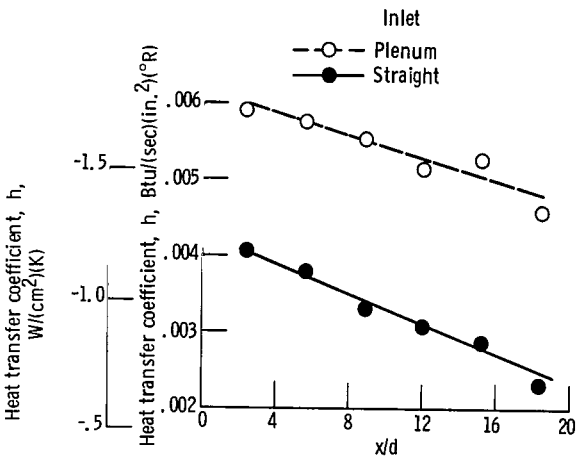

Figure 7. - Near critical hydrogen heat transfer coefficients. Absolute pressure, 300 psi (20.7x10^5 N/m^2); inlet velocity, 32 feet per second (9.8 m/sec); tube diameter, 0.31 inch (0.79 cm); heat flux, 1.07 Btu/(sec)(in.^{2}) (175 W/cm^2).

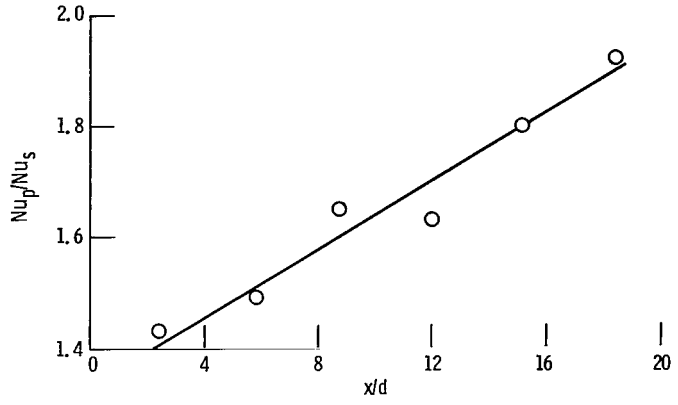

Figure 8. - Near critical hydrogen enhancement in heat transfer due to plenum inlet. Absolute pressure, 300 psi (20.7×10^5 N/m^2); inlet velocity, 32 feet per second (9.8 m/sec); tube diameter, 0.31 inch (0.79 cm); heat flux, 1.07 Btu/(sec)(in.^{2}) (175 W/cm^2).

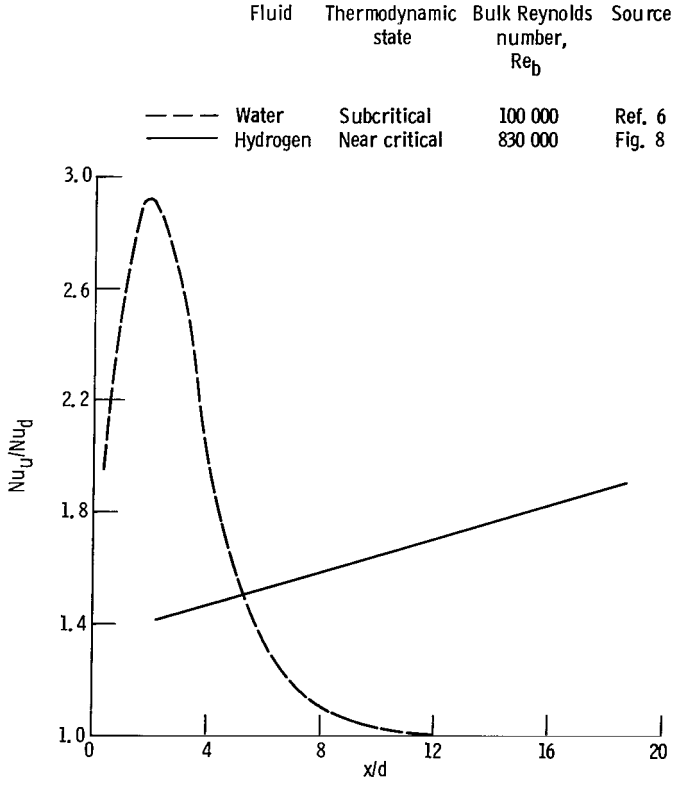

Figure 9. - Enhancement trends in heat transfer due to hydrodynamic inlet conditions.

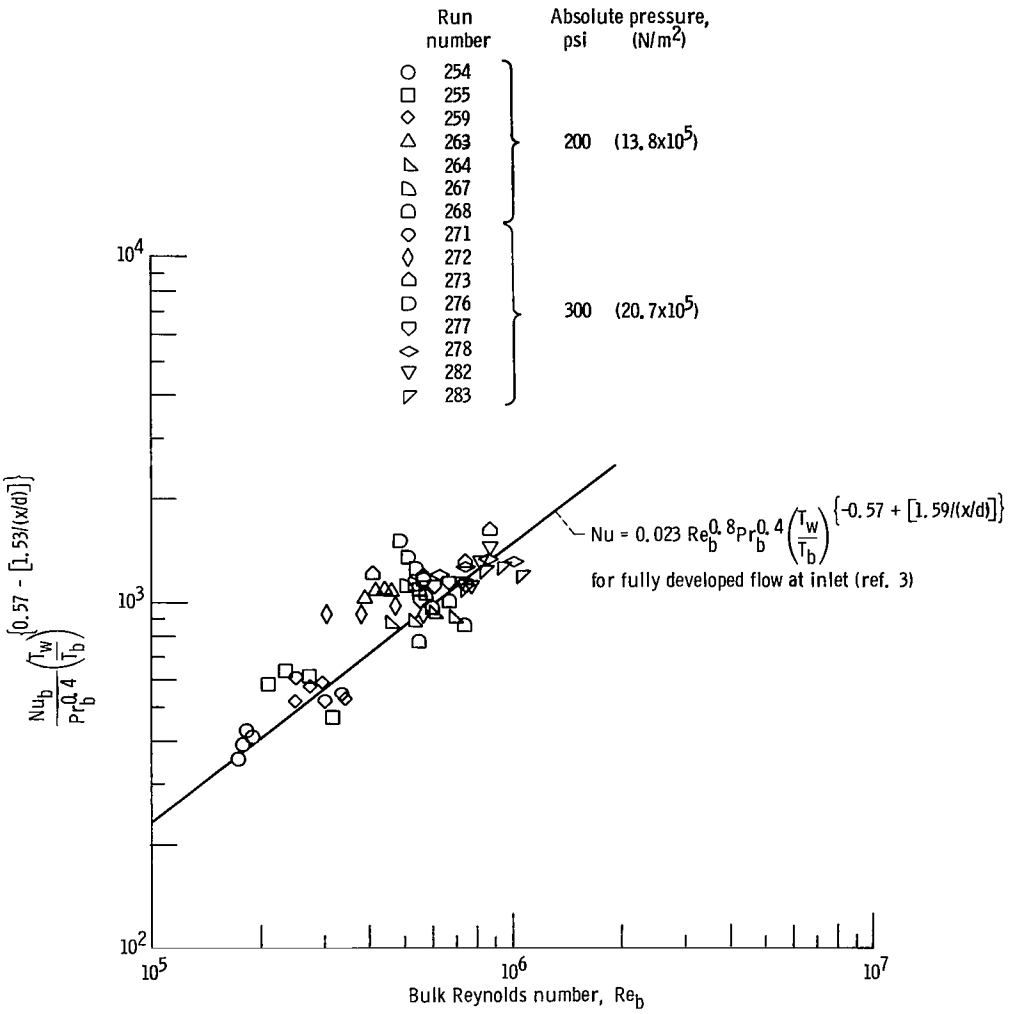

Figure 10. - Correlation of straight inlet near critical hydrogen data with equation from reference 3.

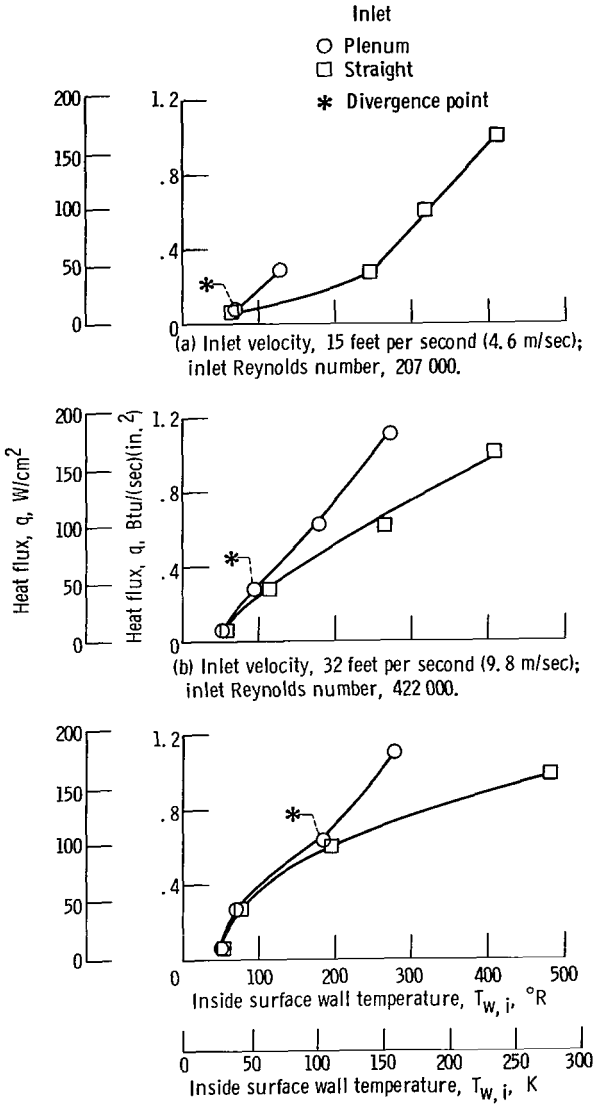

(a) Inlet velocity, 15 feet per second (4.6 m/sec); inlet Reynolds number, 207 000.

(b) Inlet velocity, 32 feet per second (9.8 m/sec); inlet Reynolds number, 422 000.

(c) Inlet velocity, 46 feet per second (14.0 m/sec); inlet Reynolds number, 592 000.

Figure 11. - Near critical hydrogen data at x/d = 15.3. Absolute pressure, 300 psi (20.7×10^5 N/m^2). (Table II).

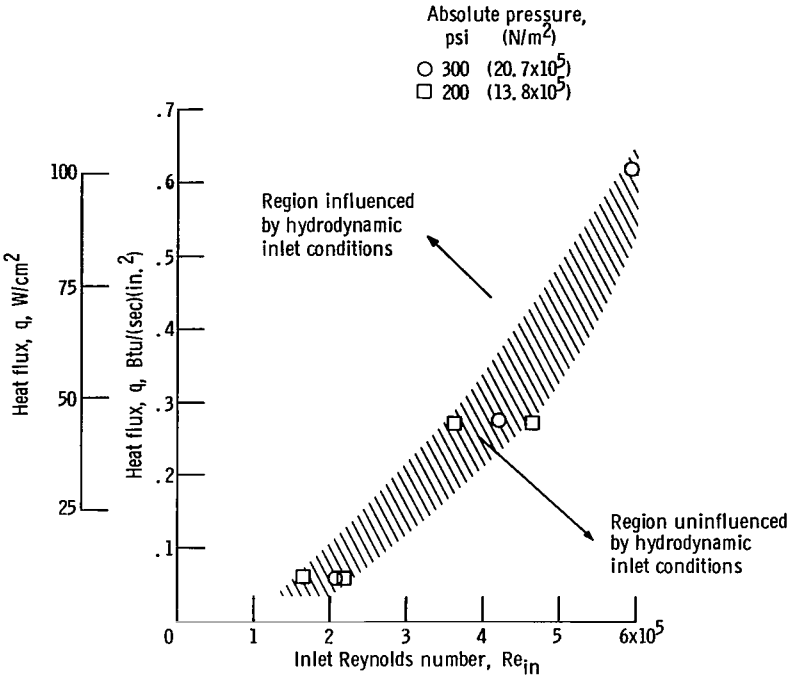

Figure 12. - Separation of near critical hydrogen data by locus of divergence points.

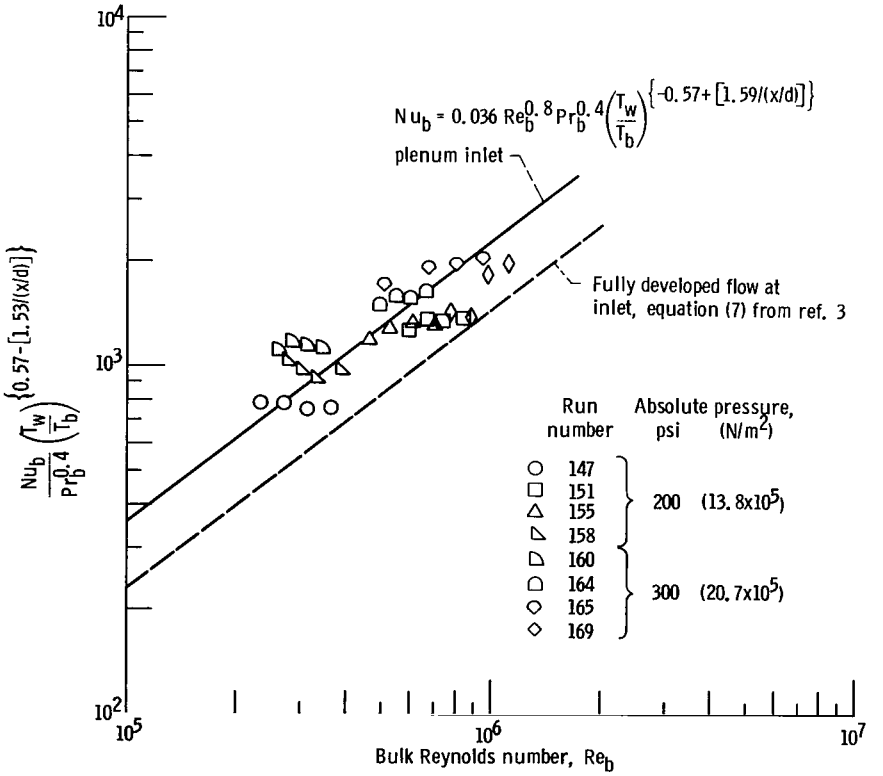

Figure 13. - Correlation of plenum inlet near critical hydrogen data influenced by hydrodynamic entrance conditions.

13U 001 37 51 3DS 71028 00903
AIR FORCE WEAPONS LABORATORY /WLOL/
KIRTLAND AFB, NEW MEXICO 87117

ATT E. LOU BOWMAN, CHIEF,TECH. LIBRARY

"The aeronautical and space activities of the United States shall be conducted so as to contribute . . . to the expansion of human knowledge of phenomena in the atmosphere and space. The Administration shall provide for the widest practicable and appropriate dissemination of information concerning its activities and the results thereof."

— NATIONAL AERONAUTICS AND SPACE ACT OF 1958

NASA SCIENTIFIC AND TECHNICAL PUBLICATIONS

TECHNICAL REPORTS: Scientific and technical information considered important, complete, and a lasting contribution to existing knowledge.

TECHNICAL NOTES: Information less broad in scope but nevertheless of importance as a contribution to existing knowledge.

TECHNICAL MEMORANDUMS: Information receiving limited distribution because of preliminary data, security classification, or other reasons.

CONTRACTOR REPORTS: Scientific and technical information generated under a NASA contract or grant and considered an important contribution to existing knowledge.

TECHNICAL TRANSLATIONS: Information published in a foreign language considered to merit NASA distribution in English.

SPECIAL PUBLICATIONS: Information derived from or of value to NASA activities. Publications include conference proceedings, monographs, data compilations, handbooks, sourcebooks, and special bibliographies.

TECHNOLOGY UTILIZATION PUBLICATIONS: Information on technology used by NASA that may be of particular interest in commercial and other non-aerospace applications. Publications include Tech Briefs, Technology Utilization Reports and Technology Surveys.

Details on the availability of these publications may be obtained from:

SCIENTIFIC AND TECHNICAL INFORMATION OFFICE

NATIONAL AERONAUTICS AND SPACE ADMINISTRATION

Washington, D.C. 20546